Circulation Research

ORIGINAL RESEARCH

Chylomicrons Regulate Lacteal Permeability and Intestinal Lipid Absorption

Georgia Zarkada,* Xun Chen,* Xuetong Zhou, Martin Lange, Lei Zeng, Wenyu Lv, Xuan Zhang, Yunhua Li, Weibin Zhou, Keli Liu, Dongying Chen, Nicolas Ricard, James Liao, Young-Bum Kim, Rui Benedito, Lena Claesson-Welsh, Kari Alitalo, Michael Simons, Rong Ju, Xuri Li, Anne Eichmann, Feng Zhang

BACKGROUND: Lymphatic vessels are responsible for tissue drainage, and their malfunction is associated with chronic diseases. Lymph uptake occurs via specialized open cell-cell junctions between capillary lymphatic endothelial cells (LECs), whereas closed junctions in collecting LECs prevent lymph leakage. LEC junctions are known to dynamically remodel in development and disease, but how lymphatic permeability is regulated remains poorly understood.

METHODS: We used various genetically engineered mouse models in combination with cellular, biochemical, and molecular biology approaches to elucidate the signaling pathways regulating junction morphology and function in lymphatic capillaries.

RESULTS: By studying the permeability of intestinal lacteal capillaries to lipoprotein particles known as chylomicrons, we show that ROCK (Rho-associated kinase)-dependent cytoskeletal contractility is a fundamental mechanism of LEC permeability regulation. We show that chylomicron-derived lipids trigger neonatal lacteal junction opening via ROCK-dependent contraction of junction-anchored stress fibers. LEC-specific ROCK deletion abolished junction opening and plasma lipid uptake. Chylomicrons additionally inhibited VEGF (vascular endothelial growth factor)-A signaling. We show that VEGF-A antagonizes LEC junction opening via VEGFR (VEGF receptor) 2 and VEGFR3-dependent PI3K/AKT activation of the small GTPase RAC1, thereby restricting RhoA/ROCK–mediated cytoskeleton contraction.

CONCLUSIONS: Our results reveal that antagonistic inputs into ROCK-dependent cytoskeleton contractions regulate the interconversion of lymphatic junctions in the intestine and in other tissues, providing a tunable mechanism to control the lymphatic barrier.

GRAPHIC ABSTRACT: A graphic abstract is available for this article.

Key Words: chylomicrons ■ endothelial cell ■ lipid ■ permeability ■ vascular endothelial growth factor

Lymphatic vessels control fluid homeostasis and immune cell trafficking in most tissues of the body and lipid absorption in the small intestine.[1–3] They form a unidirectional circulatory system with blind-ended capillaries that drain back via collecting vessels and the thoracic duct into the venous circulation. To execute their functions, lymphatic endothelial cells (LECs) lining lymphatic vessels develop 2 types of cell-cell junctions. Capillary LECs are tied together by discontinuous button-like junctions.[4] Fluids, lipids, and immune cells enter via openings between the buttons, without disrupting junctional integrity. By contrast, collector LECs have continuous, zipper-like junctions that prevent fluid leak and ensure lymph transport towards the thoracic duct, aided by smooth muscle cells and intraluminal valves.[5]

Both junction types contain the same proteins and can transform into each other via intermediate forms.[6] A few prior studies show that button junctions appear

Correspondence to: Feng Zhang, State Key Laboratory of Ophthalmology, Zhongshan Ophthalmic Center, Sun Yat-sen University, Guangdong Provincial Key Laboratory of Ophthalmology and Visual Science, Guangzhou 510060, China, Email zhangfeng@mail.sysu.edu.cn; or Anne Eichmann, Cardiovascular Research Center and Department of Cellular and Molecular Physiology, Yale University School of Medicine, New Haven, CT 06510-3221, Email anne.eichmann@yale.edu
*G. Zarkada and X. Chen contributed equally.
Supplemental Material is available at https://www.ahajournals.org/doi/suppl/10.1161/CIRCRESAHA.123.322607.
For Sources of Funding and Disclosures, see page xxx.

Circulation Research is available at www.ahajournals.org/journal/res

Novelty and Significance

What Is Known?

- Initial lymphatics at the intestine (termed lacteals) are responsible for absorption of chylomicrons, lipoprotein particles produced by enterocytes.
- Chylomicrons enter lacteals through open, button-like junctions between lymphatic endothelial cells.
- Closing (or zippering) of lymphatic endothelial cell junctions, prevents dietary lipid absorption in mice.

What New Information Does This Article Contribute?

- In newborn mice, chylomicrons trigger lacteal junction opening, following milk injection right after birth.
- Chylomicrons activate ROCK (Rho-associated kinase) signaling in lymphatic endothelial cells, remodeling junctions and allowing for lipid absorption.
- VEGF (vascular endothelial growth factor)-A signals via VEGFR (vascular endothelial growth factor receptor) 2/VEGFR3 to antagonize junction opening by suppressing ROCK.
- ROCK suppression is mediated via PI3K-dependent activation or RAC1, which inhibits RhoA.

Lymphatic vessels are essential for intestinal lipid absorption, yet the mechanisms regulating lymphatic permeability are poorly understood. Here we show that chylomicrons, lipoprotein particles produced by enterocytes, regulate their own absorption by triggering the formation of "button"-like junctions in the intestinal villus, via activation of ROCK signaling and cytoskeletal remodeling. At the same time, chylomicrons suppress VEGFR2 signaling, which limits ROCK activity by inhibiting RhoA. We show that these effects are mediated by VEGFR2/VEGFR3 heterodimer formation in response to VEGF-A, which activates the RhoA suppressor RAC1, via PI3K/AKT. This 2-pronged homeostatic mechanism ensures fat ingestion on postnatal milk consumption. In addition, we show that ROCK-mediated cytoskeletal contractions regulate lymphatic junction morphology and permeability also outside the intestine, in the mouse dermis. This study identifies lymphatic junctions as an important regulator of lymphatic vessel function, suggesting a novel target to control lipid absorption and tissue drainage in preclinical models of disease.

Nonstandard Abbreviations and Acronyms

BECs	blood vascular endothelial cells
HDLECs	human dermal lymphatic endothelial cells
HUVECs	human umbilical vein endothelial cells
LECs	lymphatic endothelial cells
MLC2	myosin light chain 2
ROCK	Rho-associated kinase
SFK	Src family kinase
VEGF	vascular endothelial growth factor
VEGFR	vascular endothelial growth factor receptor

postnatally and revert back to zippers during inflammation, indicating dynamic remodeling.[4,6] Infection-induced dermal capillary zippering inhibits dissemination of vaccinia virus,[7] identifying lymphatic junctions as critical regulators of infection resistance. Junction zippering of intestinal lymphatic capillaries termed lacteals inhibits chylomicron uptake and confers resistance to diet-induced obesity,[8] demonstrating effects of LEC junction status on whole-body metabolism. Targeting junction remodeling appears as a promising approach to control lymphatic function, but mechanisms regulating this process remain largely unknown.

We have here investigated LEC junction remodeling in the context of lipid uptake in neonatal intestine. On ingestion of breast milk after birth, the newborn mammalian gastrointestinal tract becomes a lipid-rich environment that supplies energy and essential signaling constituents.[9] Milk-derived lipids are absorbed by enterocytes and repackaged into chylomicrons, large lipoprotein particles containing triglycerides, cholesterol, and $ApoB_{48}$. Newly synthesized chylomicrons exit the abluminal side of enterocytes and are taken up by lacteals.[10] Lacteal growth inhibition via VEGF (vascular endothelial growth factor)-C/VEGFR3 inactivation, loss of lacteal DLL4/Notch activity, or loss of calcitonin receptor–like receptor (*Calcrl*), resulted in reduced chylomicron absorption.[11–16] Impaired lacteal extension into the villus, because of abnormal smooth muscle cell coverage, shifted lipid absorption from the lymphatic system to the portal circulation, leading to hepatic lipidosis.[17] This indicates that the lacteals are essential for chylomicron uptake and transport.

Here, we show that newborn lacteal junctions open in response to ingested lipids that trigger their own absorption by activating ROCK-dependent cytoskeletal pull. Chylomicrons also inhibit intestinal VEGF-A signaling by upregulating the VEGF-A decoy receptor VEGFR1 in blood vascular endothelial cells (BECs) via $ApoB_{48}$.[8,18] We show that VEGF-A antagonizes junction opening via VEGFR2/VEGFR3-dependent PI3K activation of the

small GTPase RAC1, which inhibits RhoA/ROCK–mediated cytoskeleton contraction. Our findings thus reveal that ROCK-dependent cytoskeleton remodeling controls the permeability of lymphatic junctions in response to environmental cues.

METHODS

Data Availability

The RNA-sequencing data from human umbilical vein endothelial cells (HUVECs) and human dermal LECs (HDLECs) are available in the NCBI Gene Expression Omnibus database (accession numbers GSE209855 and GSE212743). All data are included in the article and the Supplemental Material. Additional information can be obtained from the corresponding authors on reasonable request.

Detailed methods can be found in the Supplemental Material.

Mice

Vegfr2^{Y949F}[19] and *Akt1*$^{-/-}$*20* mice were described previously. *Vegfr2*$^{flox/flox}$[21] *Vegfr3*$^{flox/flox}$[22] *PLCγ 1*$^{flox/flox}$[23] *Erk1*$^{-/-}$ (JAX Strain no. 019113), *Erk2*$^{flox/flox}$ (JAX Strain no. 019112), *Rock1*$^{flox/flox}$[24] and *Rock2*$^{flox/flox}$[25,26] and *iMB-Vegfr2* mice[27] mice were intercrossed with *Prox1CreER*^{T2} mice.[28] All mice were on a C57BL/6J background and housed in pathogen-free animal facilities with a 12-hour/12-hour light-dark cycle. Mice of both sexes were used. Animal experiments were approved by the Institutional Animal Care and Use Committees of Yale University and Zhongshan Ophthalmic Center, Sun Yat-sen University.

To induce postnatal gene recombination, we injected mice intraperitoneally or intragastrically with tamoxifen (no. T5648; 20 mg/mL in corn oil; Sigma). Postnatal mice received 75 µg/g tamoxifen daily for 3 days between postnatal day (P) 0 and P2, P5 and P7, or P16 and P18 (intraperitoneally or intragastrically). Adult mice received 2 mg tamoxifen on days 1, 2, 3, 5, and 7, starting at age week 5 (intraperitoneally). All *Rock1/2iLKO* mice were analyzed within 2 weeks after the first tamoxifen injection. tamoxifen-injected Cre-negative littermates were used as controls.

Statistics

For statistical analysis, we used Prism 9-GraphPad software. For comparisons of mouse phenotypes, multiple measurements per mouse were averaged before statistical analysis. We analyzed at least 4 mice per condition and mouse numbers per experiment are indicated in figure legends. Animals were included based on genotypes, proper age, and sex. In some experiments, mice were randomly divided into groups to receive different treatments. For Western blot quantifications, protein expression was normalized to endogenous control expression, to correct for loading variation between samples. All time points/conditions were then normalized to the average value of baseline/control measurements. Changes were compared using the appropriate statistical test, as indicated in figure legends for each experiment.

For 2 group comparisons data were subjected to the nonparametric Mann-Whitney *U* test. For multiple group comparisons data were analyzed either by 1-way ANOVA (data with equal variances) followed by the Tukey post hoc test, or by Welch ANOVA (data with unequal variances) followed by the Dunnett T3 post hoc test. For ANOVA, normal distribution was determined using the Shapiro-Wilk test. $P<0.05$ was considered statistically significant. Data are expressed as mean±SEM along with scatter plots of individual data points. Each dot represents one mouse or one experiment, as described in the figure legends. No outliers were excluded.

RESULTS

Chylomicron-Induced Cytoskeletal Contraction Opens Lacteal Junctions via ROCK

To assess the status of perinatal lacteal junctions, intestinal villi in mouse jejunum were stained for the junctional marker VE-Cadherin (vascular endothelial cadherin; Figure 1A) and the junctions were categorized as buttons or zippers based on their morphology (Figure 1B, see Methods). Lacteals from nonfed prenatal embryonic day 20.5 mice displayed predominantly (>85%) continuous, zipper-like junctions (Figure 1A through 1C). By contrast, milk-fed P0.5 mice exhibited significantly fewer (<50%) zipper junctions and more discontinuous, button-like junctions (Figure 1A through 1C). As the appearance of discontinuous, presumably open LEC junctions, coincided with lacteal exposure to chylomicrons, we asked if the chylomicrons affected junction opening. in vitro, confluent LECs cultured in complete media displayed continuous, straight VE-cadherin (vascular endothelial cadherin)$^{+}$ adherens junctions, likely due to the presence of VEGF-A in fetal bovine serum.[8] On chylomicron exposure, the junctions transformed into discontinuous, parallel linear segments of VE-cadherin, connected to radial actin stress fibers via focal vinculin-positive patches (Figure 1D). Treatment with arachidonic acid, the most common long-chain polyunsaturated fatty acid in human milk,[29] mimicked the effects of chylomicrons on LECs (Figure 1D). The effect was observed at 30 minutes and disappeared at 120 minutes (Figure 1D). The appearance of junction-anchored actin stress fibers suggested increased cytoskeletal contraction, as attested by increased phosphorylation of MLC2 (myosin light chain 2) in response to chylomicrons or arachidonic acid treatment, compared with untreated cells (Figure 1E through 1H). In vivo, wild-type lacteal VE-Cadherin^{+} discontinuous junctions colocalized with the tension sensor vinculin (Figure 1I), leading us to hypothesize that chylomicron-derived lipids promote junction opening by triggering cytoskeletal tension changes in lacteal LECs.

Lipids such as arachidonic acid can activate ROCK, the major regulator of cytoskeletal contraction, in a RhoA-dependent or independent manner,[30–34] and pharmacological ROCK inhibition zippered lacteal junctions and prevented chylomicron uptake in postnatal mice.[8] This suggested that lipid-activated ROCK

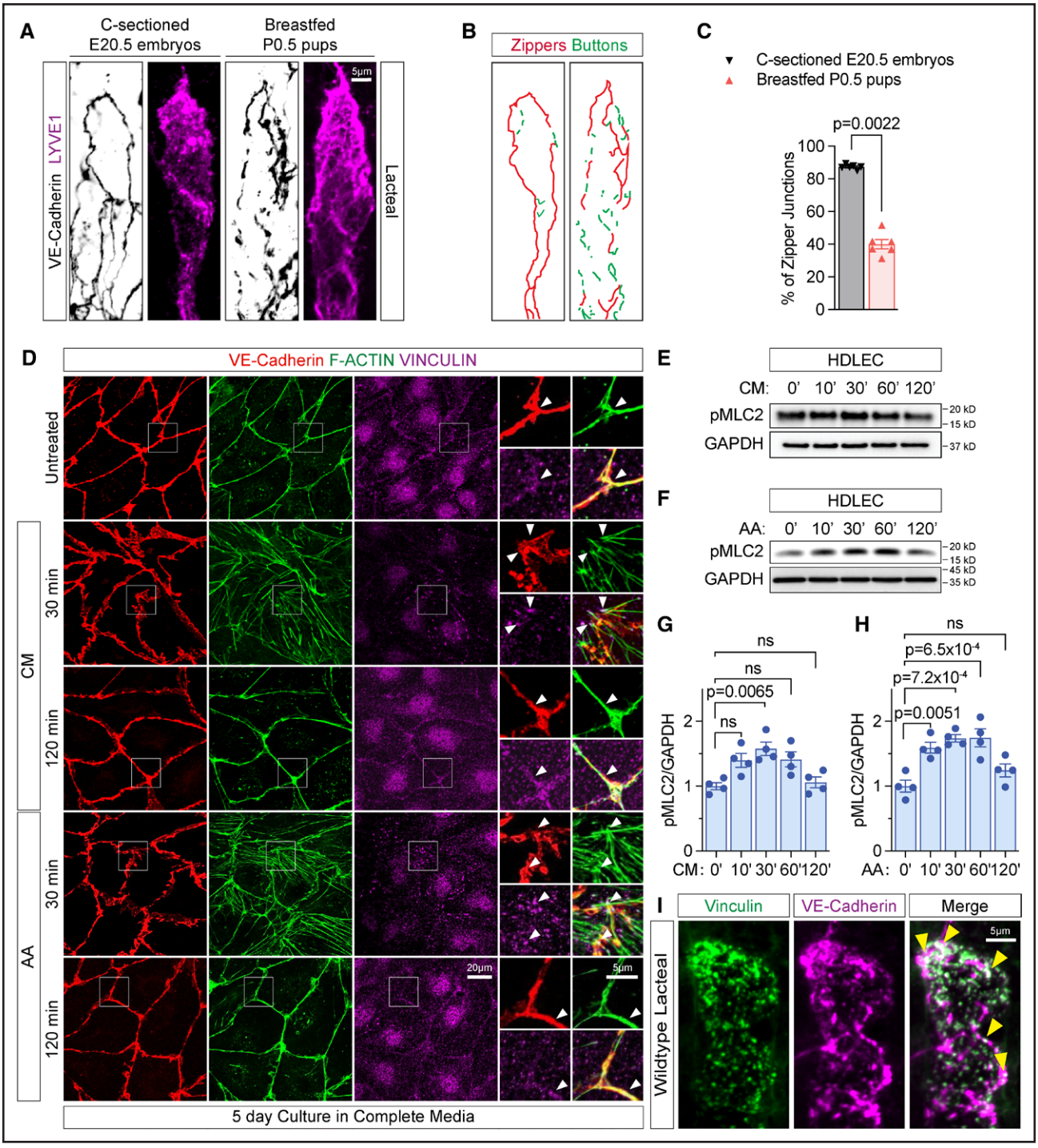

Figure 1. Chylomicrons and lipids promote lacteal junction opening via cytoskeletal contractions.
A, VE-Cadherin (vascular endothelial cadherin) and LYVE1 staining of jejunum lacteals of C-sectioned embryonic day (E) 20.5 wild-type mouse embryos and breastfed postnatal day (P) 0.5 neonatal pups. **B**, Example of junction morphology quantification from **A**. The length of zipper and button-like junctions is annotated in green and red respectively and measured using Fiji software (see online Methods). **C**, Quantification of % zipper-like junctions out of total junction length in lacteals shown in **A**. Each symbol represents one mouse. N=6 mice per group. Error bars, SEM. Mann-Whitney *U* test. **D**, VE-Cadherin, F-actin, and Vinculin staining of confluent human dermal lymphatic endothelial cells (HDLECs) in complete media with or without treatment with 50 μg/mL chylomicrons (CM) or 30 μM arachidonic acid (AA) at the indicated time points. Arrowheads indicate colocalization of VE-Cadherin, F-actin, and Vinculin staining at junctional sites. **E** through **H**, Western blot and quantification of pMLC2 (Thr18/Ser19), normalized to GAPDH, in HDLECs treated with 50 μg/mL CM (**E** and **G**) or 30 μM AA (**F** and **H**) at indicated time points. Data are expressed as fold changes compared with the average value of time (T)=0′. N=4 experiments. Error bars, SEM. One-Way ANOVA with post hoc Tukey test. **I**, VE-Cadherin, vinculin, and LYVE1 staining of jejunum lacteals of wild-type mice. Arrowheads point to VE-cadherin and Vinculin colocalization on button-like structures.

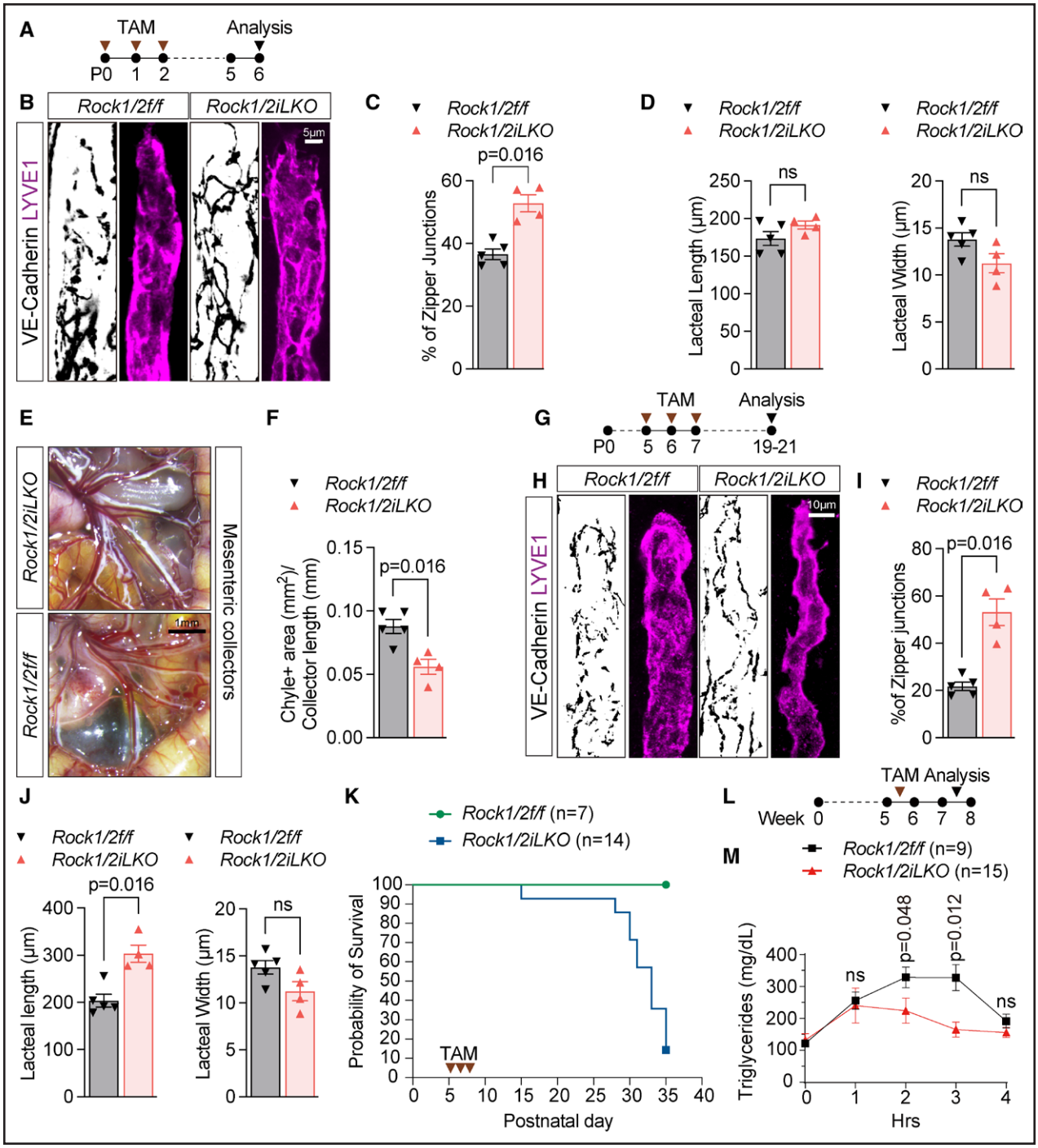

Figure 2. ROCK (Rho-associated kinase) is required for lacteal junction opening and lipid uptake.

A, Experimental strategy to induce *Rock1/2* deletion in **B**–**F**. Arrowheads represent 3X75 μg/g tamoxifen (TAM) injections, followed by analysis at postnatal day (P) 6. **B**, VE-Cadherin (vascular endothelial cadherin) and LYVE1 staining of jejunum lacteals from P6 *Rock1/2f/f* and *Rock1/2iLKO* mice. **C** and **D**, Quantification of % lacteal zipper-like junctions normalized to total junction length, and lacteal length and width of P6 *Rock1/2f/f* and *Rock1/2iLKO* mice. Each dot represents one mouse. N=4 or 5 mice per group. Error bars, SEM. ns, not significant. Mann-Whitney *U* test. **E** and **F**, Images of mesenteries and quantification of chyle-filled lymphatic collectors of P6 *Rock1/2f/f* and *Rock1/2iLKO* mice. Each dot represents one mouse. N=4 or 5 mice per group. Mann-Whitney *U* test. **G**, Experimental strategy to induce *Rock1/2* deletion in **H**–**J**. Arrowheads represent 3×75 μg/g TAM injections, followed by analysis at P19–P21. **H**, VE-Cadherin and LYVE1 staining of jejunum lacteals from P19 to P21 *Rock1/2f/f* and *Rock1/2iLKO* mice. **I** and **J**, Quantification of % lacteal zipper-like junctions, normalized to total junction length, and lacteal length and width from P19 to 21 *Rock1/2f/f* and *Rock1/2iLKO* mice. Each dot represents one mouse. N=4 or 5 mice per group. Error bars, SEM. Mann-Whitney *U* test. **K**, Survival curves of *Rock1/2f/f* and *Rock1/2iLKO* mice after 3×75 μg/g TAM injections at P5, P6, and P7. N=7 or 14 mice per group. **L** and **M**, Timeline of TAM administration (2 mg/day for 5 days) and plasma triglyceride measurements of adult *Rock1/2f/f* and *Rock1/2iLKO* mice. Mice were fasted for 6 hours, gavaged with 200 μL of olive oil, and plasma triglycerides were measured. N=9 or 15 mice per group. Error bars, SEM. Mann-Whitney *U* test was performed to compare *Rock1/2f/f* and *Rock1/2iLKO* groups at the same time points.

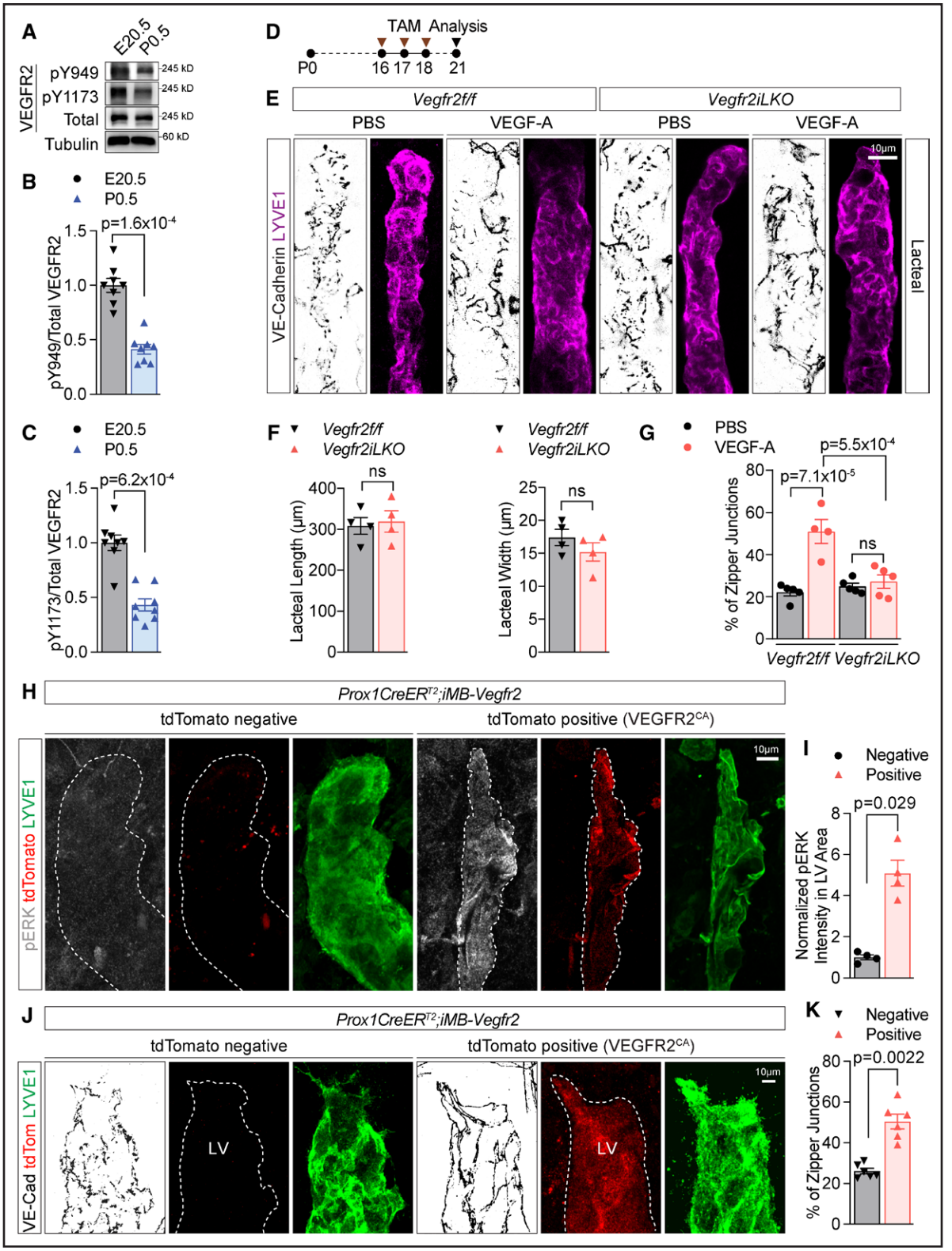

Figure 3. VEGFR (vascular endothelial growth factor receptor) 2 activation zippers lymphatic capillary junctions.
A through **C**, Western blot and quantifications of phospho-VEGFR2 (pY949 and pY1173), normalized to total VEGFR2, in jejunum tissue lysates from nonfed prenatal embryonic day (E) 20.5 and milk-fed postnatal day (P) 0.5 mice. Data are expressed as fold changes compared with the average value of E20.5. Each dot represents one mouse. N=8 mice per group. Error bars, SEM. Mann-Whitney *U* test. **D**, Experimental strategy to induce *Vegfr2* deletion or overexpression, shown in **E**–**K**. Arrowheads represent 3×75 μg/g tamoxifen (TAM) injections, followed by analysis at P21. **E**, VE-Cadherin (vascular endothelial cadherin) and LYVE1 staining of jejunum lacteals from P21 *Vegfr2f/f* and *Vegfr2iLKO* mice 30 minutes after intravenous injection of PBS or 250 ng/g VEGF-A. **F**, Quantifications of jejunum lacteal length and width in P21 *Vegfr2f/f* and (*Continued*)

signaling could regulate lacteal permeability. In cultured LECs, serum starvation induced the formation of discontinuous VE-Cadherin$^+$ adherens junctions. Silencing of both mammalian ROCK isoforms, *ROCK1* and *2*,[35] reverted these junctions back into straighter ones, confirming a LEC-autonomous role for ROCK in zippering lymphatic junctions (Figure S1A). To determine this effect in vivo, we generated LEC-specific ROCK conditional mutant mice by intercrossing *Rock1*$^{flox/flox}$, *Rock2*$^{flox/flox}$, and *Prox1CreER*^{T2} mice (*Prox1CreER*^{T2}*;Rock1*$^{flox/flox}$*;Rock2*$^{flox/flox}$: *Rock1/2iLKO*).[24–26,28] Tamoxifen administration to these mice reduced ROCK1 and 2 protein expression significantly in initial lymphatics, confirming LEC-specific gene deletion (Figure S1B and S1C). Analysis of P6 *Rock1/2iLKO* mice that had been administered tamoxifen at P0-P2 revealed straight zipper-like junctions in jejunal lacteals, whereas Cre-negative littermate controls (*Rock1*$^{flox/flox}$*;Rock2*$^{flox/flox}$*: Rock1/2f/f*) had mainly discontinuous button-like junctions (Figure 2A through 2C). Lacteal length or width were not significantly altered in the mutants (Figure 2D). Functionally, the P6 *Rock1/2iLKO* pups had significantly less chyle in their mesenteric lymphatic vessels than their littermate controls (Figure 2E and 2F), attesting to functional defects in chyle transport. To investigate whether ROCK1/2 loss of function affects button maintenance, we analyzed P19 to P21 *Rock1/2iLKO* mice after tamoxifen administration between P5 and P7 (Figure 2G). These mice exhibited more lacteal zipper junctions than control littermates (Figure 2H and 2I), plus increased length and unaltered width of lacteals (Figure 2J), and lethality by P35 due to as yet undetermined causes (Figure 2K). The increase of blood triglyceride levels was also suppressed in adult mutant mice that received olive oil gavage 10 days after completion of tamoxifen administration (Figure 2L and 2M). Taken together, our results show that ROCK activity in LECs is required for the formation and maintenance of lacteal button junctions, and for fat uptake in the gastrointestinal tract.

LEC VEGFR2 Activation Zippers Lymphatic Capillary Junctions

An increase of VEGF-A bioavailability or exogenous VEGF-A administration can zipper initial lymphatics, and chylomicrons are known to suppress VEGF-A signaling by upregulating the VEGF-A decoy receptor VEGFR1 in BECs via $ApoB_{48}$.[8,18] In line with this, VEGFR2 phosphorylation was significantly reduced in jejunum from milk-fed P0.5 mice, compared with nonfed prenatal embryonic day 20.5 mice (Figure 3A through 3C). To determine if this process required LEC-autonomous VEGFR2 signaling, we produced LEC-specific inducible *Vegfr2* knockout mice (*Prox1CreER*^{T2}*;Vegfr2*$^{flox/flox}$: *Vegfr2iLKO*).[21] Tamoxifen administration between P16-18 abolished VEGFR2 protein expression in *Vegfr2iLKO* lacteals (Figure S2A through S2C). Loss of *Vegfr2* from the lymphatics did not affect lacteal junction morphology, or lacteal length or width at baseline conditions (Figure 3D through 3F). However, intravenous VEGF-A injection increased the ratio of lacteal zipper- versus button-like junctions in control mice, but not in *Vegfr2iLKO* mice (Figures 3E and 3G).

In a complementary VEGFR2 gain-of-function approach, we investigated the effects of VEGFR2 activation on junction morphology by using *Prox1CreER*^{T2}*-iMb-Vegfr2*. On tamoxifen treatment, these mice express either a tdTomato-tagged VEGFR2 with constitutive ligand-independent kinase activity, or a YFP (yellow fluorescent protein) fused dominant negative VEGFR2, or a far-red fluorescent mKate2[27] in stochastically recombined LECs. Since tissue preparation diminished strong tdTomato signals in the lacteals, we analyzed initial lymphatics in the dermis. As predicted, tamoxifen administration led to LEC-specific expression of red tdTomato fluorescence in a subset of dermal initial lymphatics, along with significantly increased ERK (extracellular signal-regulated kinase) phosphorylation, confirming VEGFR2 overactivation (Figure 3H and 3I). We found more zippered junctions in tdTomato-positive than tdTomato-negative LECs (Figure 3J and 3K). Taken together, our data show that LEC VEGFR2 signaling is dispensable for junction opening at baseline, whereas its activation is sufficient to zipper junctions.

VEGFR2 Y949 Phosphorylation Is Dispensable for Modulation of Lacteal Junctions

Next, we addressed the mechanisms of VEGF-A/VEGFR2 induced LEC junction zippering. VEGF-A-induced permeability in BECs is regulated by phosphorylation of VEGFR2 at tyrosine (Y) 949, which mediates the binding of VEGFR2 to the Src homology 2-domain of TSAd (T-cell–specific adaptor), leading to c-Src

Figure 3 Continued. *Vegfr2iLKO* mice. Error bars, SEM. Each dot represents one mouse. N=4 mice per group. ns, not significant. Mann-Whitney *U* test. **G**, Quantification of % zipper-like junctions out of total junction length in lacteals shown in **E**. Each symbol represents one mouse. N=4 or 5 mice per group. Error bars, SEM. One-Way ANOVA with post hoc Tukey test. **H**, pERK and LYVE1 staining of VEGFR2^{CA}-tdTomato (+) and (—) ear dermal lymphatic capillaries of P21 *iMB-Vegfr2;Prox1CreER*^{T2} mice. **I**, Quantification of pERK intensity in VEGFR2^{CA}-tdTomato (+) and (—) lymphatic vessels outlined in **H**. Each dot represents one mouse. N=4 mice per group. Error bars, SEM. Mann-Whitney *U* test. **J**, VE-Cadherin, tdTomato and LYVE1 staining of ear dermal lymphatic capillaries from P21 *iMB-Vegfr2;Prox1CreER*^{T2} mice. **K**, Quantification of zipper-like lymphatic junctions out of total lymphatic junction length in VEGFR2^{CA}-tdTomato (+) and (—) lymphatic vessels in **J**. Each dot represents one mouse. N=6 mice per group. Error bars, SEM. Mann-Whitney *U* test. CA indicates constitutive active; and LV, lymphatic vessel.

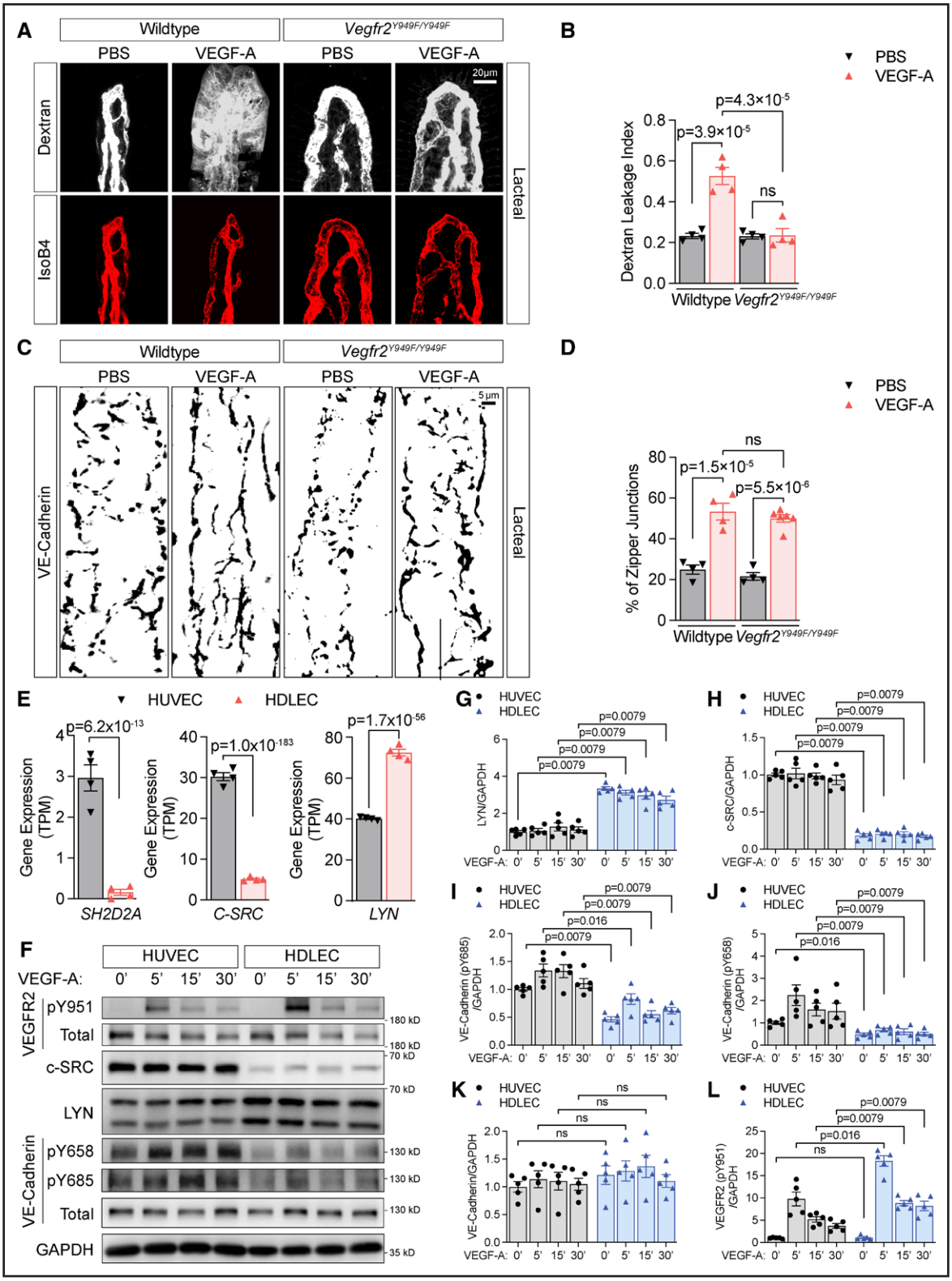

Figure 4. VEGFR (VEGF [vascular endothelial growth factor] receptor) 2 Y949 regulates permeability in blood but not in lymphatic vessels.

A, Dextran leakage of jejunum villus blood vessels in postnatal day (P) 11 to P13 *Vegfr2*$^{Y949F/Y949F}$ mice and wild-type littermates, 10 minutes after retro-orbital injection of fluorescent labeled IsoB4/dextran (70 kDa) with 250 ng/g VEGF-A or PBS. **B**, Quantification of dextran leakage shown in **A**. Each symbol represents one mouse. N=4 mice per group. Error bars, SEM. One-Way ANOVA with post hoc Tukey test. **C**, VE-Cadherin (vascular endothelial cadherin) staining of jejunum lacteals from P21 wild-type and *Vegfr2*$^{Y949F/Y949F}$ mice 30 minutes after intravenous injection of PBS or 250 ng/g VEGF-A. **D**, Quantification of % zipper-like junctions out of total junction length in lacteals shown in **C**. Each symbol (*Continued*)

activation, and increased VE-Cadherin phosphorylation. This mechanism disrupts adherens junctions and increases vascular permeability.[19,36] We tested whether Y949 is involved in LEC junction remodeling by analyzing junction morphology in *Vegfr2*$^{Y949F/Y949F}$ mice that carry a Y to F (phenylalanine) substitution at position 949, which blocks VEGF-A induced permeability.[19] Blood vascular leakage and extravasation of fluorescent dextran after intravenous injection of VEGF-A were prevented in the *Vegfr2*$^{Y949F/Y949F}$ mutant intestinal vasculature (Figure 4A and 4B), confirming BEC permeability regulation via Y949. However, LEC junctions were not affected, as VEGF-A injection increased the number of zipper-like junctions to the same extent in control and *Vegfr2*$^{Y949F/Y949F}$ mice (Figure 4C and 4D). Thus, Y949 signaling does not regulate LEC junction morphology downstream of VEGFR2.

Bulk RNA-sequencing revealed very low *SH2D2A* (encoding TSAd) expression in HDLECs versus HUVECs (Figure 4E). Interestingly, we observed a significant decrease in C-SRC transcripts and protein in HDLECs versus HUVECs, while another SFK (Src family kinase) *LYN* was significantly increased (Figure 4E through 4H). The YES1 and FYN SFK protein levels were not changed despite mild to moderate increase of their transcripts in HDLECs versus HUVECs (Figure S3A through S3D). In BECs in vivo, phosphorylation of VE-Cadherin at Y658 and Y685 mediates junction opening downstream of SFKs.[37,38] Signaling studies revealed that the VEGF-A–induced phosphorylation of VE-Cadherin at Y685 and Y658 was profoundly reduced in HDLECs versus HUVECs, despite robust phosphorylation of VEGFR2 Y951 (the human Y949 homolog; Figure 4F through 4L). Thus, intrinsic differences in TSAd/SFKs expression between BECs and LECs could account for the differential responses to VEGF-A activation and VE-Cadherin phosphorylation in BECs versus LECs, and explain why LECs do not remodel their junctions in response to Y949 phosphorylation.

VEGFR3 Is Required for VEGF-A Induced Lacteal Junction Zippering

VEGFR3 is the main receptor involved in lymphangiogenesis and lymphatic maintenance.[39] VEGFR3 binds VEGF-C and VEGF-D, but not VEGF-A.[40] To determine if VEGFR3 regulates LEC junctions, we generated lymphatic specific *Vegfr3* mutants by crossbreeding *Vegfr3* floxed mice[22] with *Prox1CreER*^{T2} mice *(Prox1CreER*^{T2}*;Vegfr3*$^{flox/flox}$*: Vegfr3iLKO).* Deletion of *Vegfr3* dramatically decreased lacteal length (Figure S4A and S4B), in line with previous reports.[41] We, therefore, opted for a short deletion window that did not affect the ratio of lacteal zipper/button junctions at baseline conditions or lacteal length, although it minimally decreased lacteal width (Figure 5A through 5E). Intriguingly, although VEGF-A injection increased the number of lacteal zipper-like junctions in control mice, *Vegf3iLKO* mice maintained mostly buttoned junctions (Figure 5B and 5C). As VEGFR3 does not bind VEGF-A directly, we hypothesized that VEGFR3 either modulates VEGFR2 expression levels, or VEGFR2 signaling output via the formation of VEGFR2/VEGFR3 heterodimers.[42,43] We did not observe any changes in VEGFR2 protein levels in lacteals of *Vegfr3iLKO* mice (Figure 5F and 5G), or any changes to *VEGFR2* mRNA levels in cultured LECs after silencing *VEGFR3* (Figure 5H). However, silencing of *VEGFR3* in HDLECs reduced AKT phosphorylation in response to VEGF-A, whereas phosphorylation of Y951, Y1175, Y1214, and ERK remained unchanged (Figure 5I and 5J). These results suggested that VEGFR3 contributes to LEC junction zippering by reinforcing PI3K/AKT signaling downstream of VEGF-A/VEGFR2, presumably via the formation of VEGFR2/VEGFR3 heterodimers.

VEGF-A Zippers Lacteal Junctions via PI3K/AKT Signaling

To determine PI3K/AKT signaling requirement for lacteal junction zippering in vivo, we analyzed *Akt1* mouse mutants (*Akt1*$^{-/-}$*: Akt1KO*).[20] Global loss of *Akt1* did not affect junction morphology or lacteal length or width (Figure 6A through 6D). Intravenous VEGF-A injection increased the number of zipper-like junctions in control mice, whereas *Akt1KO* mice were resistant to VEGF-A–induced zippering (Figure 6A and 6B). Similar results were observed when we treated the mice with the PI3K inhibitor Wortmannin that blocks VEGF-A–induced phosphorylation of AKT (Figure 6A and 6B; Figure S5A and S5B). In parallel, we investigated the role of PLCγ-ERK pathway downstream of VEGFR2 Y1175 phosphorylation.[44] We analyzed lymphatic specific mutants of *Plcγ 1* (*Prox1CreER*^{T2}*;Plcγ 1*$^{flox/flox}$: *Plcγ 1iLKO*),[23] as well as compound mutants of *Erk1/2* (*Erk1*$^{-/-}$*;Prox1CreER*^{T2}*;Erk2*$^{flox/flox}$: *Erk1KO;Erk2iLKO*). *Plcγ 1iLKO* and

Figure 4 Continued. represents one mouse. N=4 or 6 mice per group. Error bars, SEM. One-Way ANOVA with post hoc Tukey test. **E**, RNA-sequencing analysis of *SH2D2A* (encoding TSAd [T-cell–specific adaptor]), *C-SRC*, and *LYN* differential expression in cultured human dermal lymphatic endothelial cells (HDLECs) vs human umbilical vein endothelial cells (HUVECs). Shown are transcript per million values of the indicated genes. N=4 experiments. Error bars, SEM. Benjamini-Hochberg test. **F**, Western blot analysis for the indicated proteins in HDLECs vs HUVECs treated with 50 ng/mL VEGF-A for 0, 5, 15, and 30 minutes. **G** through **L**, Quantifications of the protein blots, normalized to GAPDH, shown in **F**. Data are expressed as fold changes compared with the average value of T=0′ of HUVEC group. Error bars, SEM. N=5 experiments. Mann-Whitney *U* test was performed to compare HDLECs vs HUVECs at the same time points.

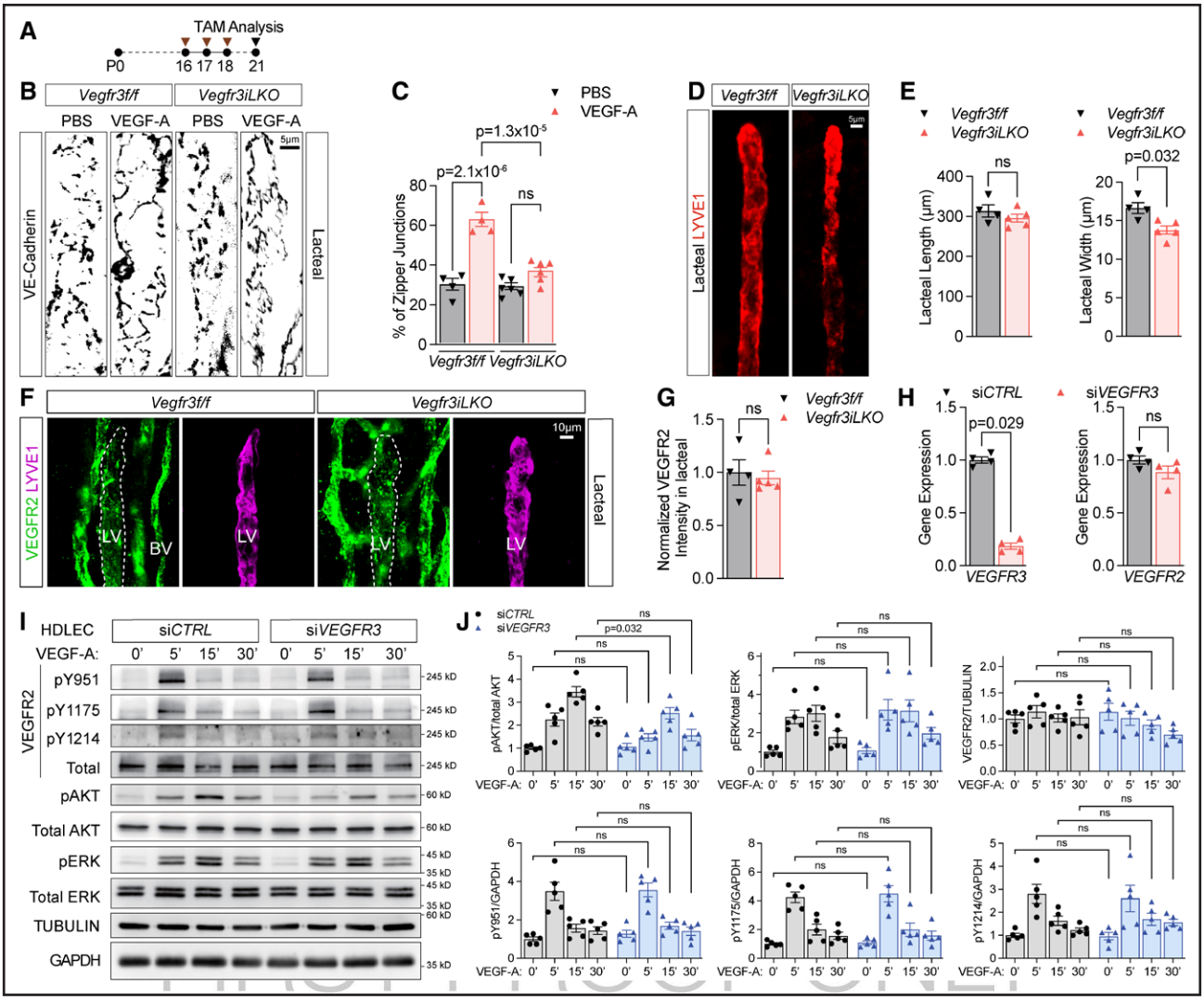

Figure 5. VEGFR (VEGF [vascular endothelial growth factor] receptor) 3 is required for VEGF-A/VEGFR2–induced lymphatic junction zippering.

A, Timeline of experiments shown in **B**–**G**. Arrowheads represent 3×75 μg/g tamoxifen (TAM) injections and analysis at postnatal day (P) 21. **B**, VE-Cadherin (vascular endothelial cadherin) staining of jejunum lacteals from P21 *Vegfr3f/f* and *Vegfr3iLKO* littermates, 30 minutes after PBS or 250 ng/g VEGF-A intravenous injection. **C**, Quantification of % zipper-like junctions out of total junction length in lacteals shown in **B**. Each symbol represents one mouse. N=4 or 6 mice per group. Error bars, SEM. One-way ANOVA with post hoc Tukey test. **D**, LYVE1 staining of jejunum lacteals of P21 *Vegfr3f/f* and *Vegfr3iLKO* mice. **E**, Quantifications of lacteal width and length from **D**. Each dot represents one mouse. N=4 or 5 mice per group. Error bars, SEM. Mann-Whitney *U* test. **F**, VEGFR2 and LYVE1 staining of jejunum villi from P21 *Vegfr3f/f* and *Vegfr3iLKO* mice. **G**, Quantification of VEGFR2 intensity in the lacteals outlined in **F**. Data were normalized to the average VEGFR2 intensity of *Vegfr3f/f* lacteals. Each dot represents one mouse. N=4 or 5 mice per group. Error bars, SEM. ns, not significant. Mann-Whitney *U* test. **H**, Quantitative polymerase chain reaction analysis of *VEGFR2* and *VEGFR3* expression in human dermal lymphatic endothelial cells (HDLECs) 2 days after transfection with control (*CTRL*) or *VEGFR3* siRNA. N=4 experiments. Error bars, SEM. Mann-Whitney *U* test. **I** and **J**, Western blots and quantifications of VEGFR2, ERK (extracellular signal-regulated kinase), and AKT phosphorylation, normalized to the indicated loading controls, in HDLECs transfected with si*CTRL* or si*VEGFR3* and treated with 50 ng/mL VEGF-A for 0, 5, 15 and 30 minutes. Data are expressed as fold changes compared with the average value of T=0′ of si*CTRL* group. N=5 experiments. Error bars, SEM. ns, not significant. Mann-Whitney *U* test was performed to compare si*CTRL* vs si*VEGFR3*-treated groups at the same time points. BV indicates blood vessel; and LV, lymphatic vessel.

Erk1KO;Erk2iLKO mice showed unaltered junction morphology at baseline, and zippered their junctions in response to intravenous VEGF-A (Figure 6E through 6G), demonstrating that PI3K/AKT but not PLCγ1/ERK1/2 signaling mediates lacteal junction zippering in response to VEGF-A.

VEGF-A/VEGFR2 Signaling Suppresses RhoA in LECs via RAC1 Activation

Next, we investigated how VEGF-A/VEGFR2 interacts with RhoA/ROCK during LEC junction remodeling. Stimulation of serum-starved HDLEC monolayers with VEGF-A for 30 minutes transformed the discontinuous

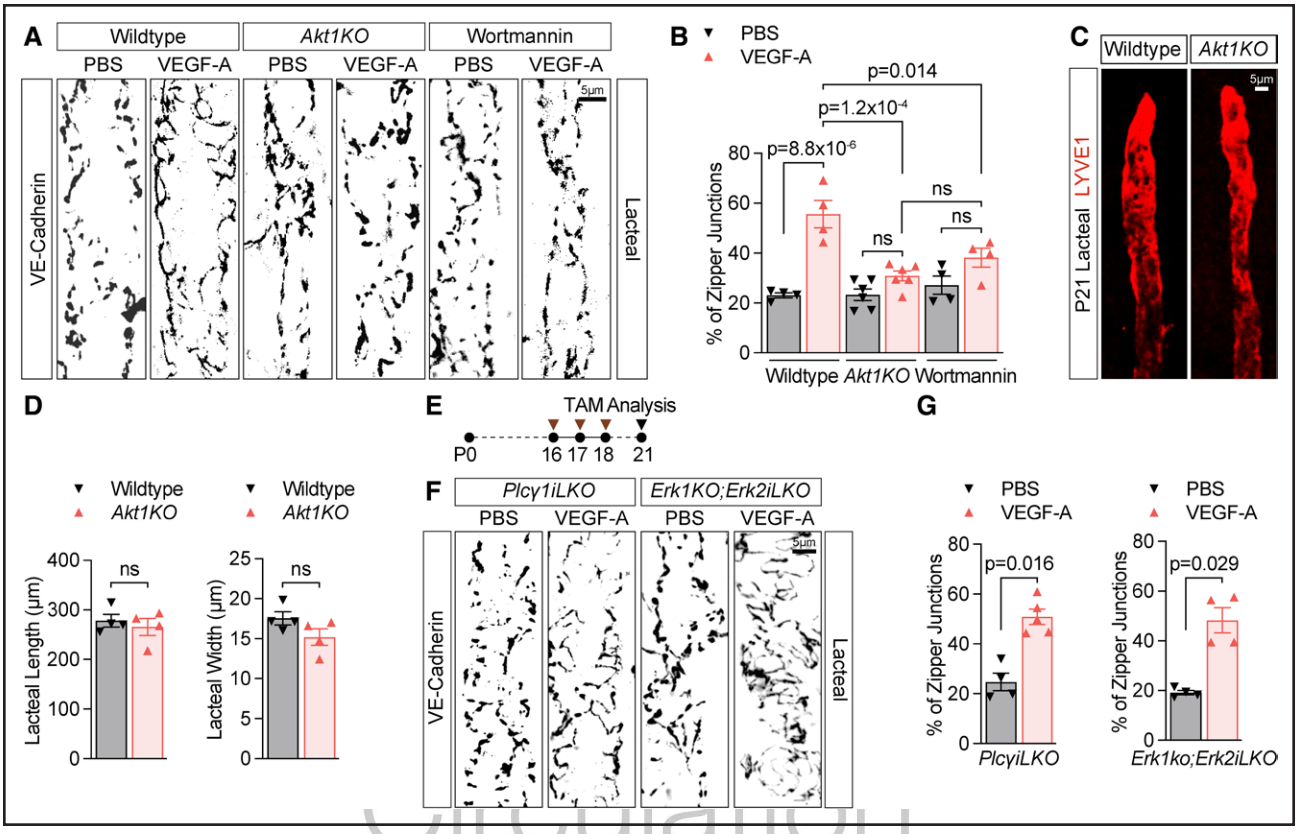

Figure 6. PI3K/AKT signaling mediates VEGF (vascular endothelial growth factor)-A–induced lymphatic junction zippering. **A**, VE-Cadherin (vascular endothelial cadherin) staining of jejunum lacteals from postnatal day (P) 21 wild-type, *Akt1KO* and Wortmannin-treated mice, 30 minutes after intravenous (IV) administration of PBS or 250 ng/g VEGF-A. **B**, Quantification of % zipper-like junctions out of total junction length in lacteals shown in **A**. Each symbol represents one mouse. N=4 or 6 mice per group. Error bars, SEM. One-Way ANOVA with post hoc Tukey test. **C**, LYVE1 staining and (**D**) quantifications of length and width of jejunum lacteals from P21 wild-type and *Akt1KO* mice. Each dot represents one mouse. N=4 mice per group. Error bars, SEM. Mann-Whitney *U* test. **E**, Experimental strategy to induce *Plcγ* or *Erk2* deletion in **F** and **G**. Arrowheads indicate 3×75 μg/g tamoxifen (TAM) injections and analysis at P21. **F**, VE-Cadherin staining of jejunum lacteals from P21 *PlcγiLKO* and *Erk1KO;Erk2iLKO* mice 30 minutes after IV injection of PBS or 250 ng/g VEGF-A. **G**, Quantification of % zipper-like junctions out of total junction length in lacteals shown in **F**. Each symbol represents one mouse. N=4–5 mice per group. Error bars, SEM. Mann-Whitney *U* test.

adherens junctions into straighter zipper junctions and reduced cytoskeletal stress fibers[8,45] (Figure 7A). Consistently, phosphorylated MLC2 was significantly decreased in HDLECs 30 minutes after VEGF-A stimulation (Figure 7B). In contrast, serum-starved HUVECs showed increased stress fiber formation and no difference in MLC2 phosphorylation 30 minutes after VEGF-A stimulation (Figure 7A and 7B). In line with the reduced pMLC2 levels in HDLECs, we found a decrease of activated, GTP-bound RhoA following VEGF-A treatment (Figure 7C). This depended on VEGFR2 since silencing of VEGFR2 sustained RhoA activity (Figure 7C). VEGF-A stimulation of HDLECs induced GTP-bound RAC1, another small GTPase of the Rho family, in a VEGFR2-dependent manner (Figure 7D). As RAC1 inactivates RhoA/ROCK, this could explain the reduced RhoA activity and actin depolymerization observed in VEGF-A–stimulated HDLECs.[46] VEGFR2-mediated RAC1 activation depended on PI3K, as pretreatment with the PI3K inhibitor Wortmannin completely abolished the elevation in RAC1-GTP levels after VEGF-A stimulation (Figure 7E). Thus, VEGF-A/VEGFR2 signaling in LECs reduces stress fiber formation by inhibiting RhoA/ROCK/MLC2 via activation of RAC1, in a PI3K-dependent manner.

ROCK Regulates Lymphatic Junction Morphology in Dermal Initial Lymphatics

To address whether VEGF-A and ROCK signaling control junction remodeling outside the gastrointestinal tract, we analyzed junction morphology in dermal lymphatic capillaries. Intradermal injection of VEGF-A–induced junction zippering in the dermal initial lymphatics of the ear[8] (Figure 8A and 8B), whereas other vascular permeability inducers, such as histamine or bradykinin, did not induce junction zippering (Figure 8A and 8B). ROCK signaling was also required for the maintenance of button junctions in dermal initial lymphatics, as *Rock1/2iLKO* mutants displayed predominantly zipper junctions at baseline (Figure 8C through 8E). To examine whether button morphology is necessary for fluid uptake, we injected Evans Blue

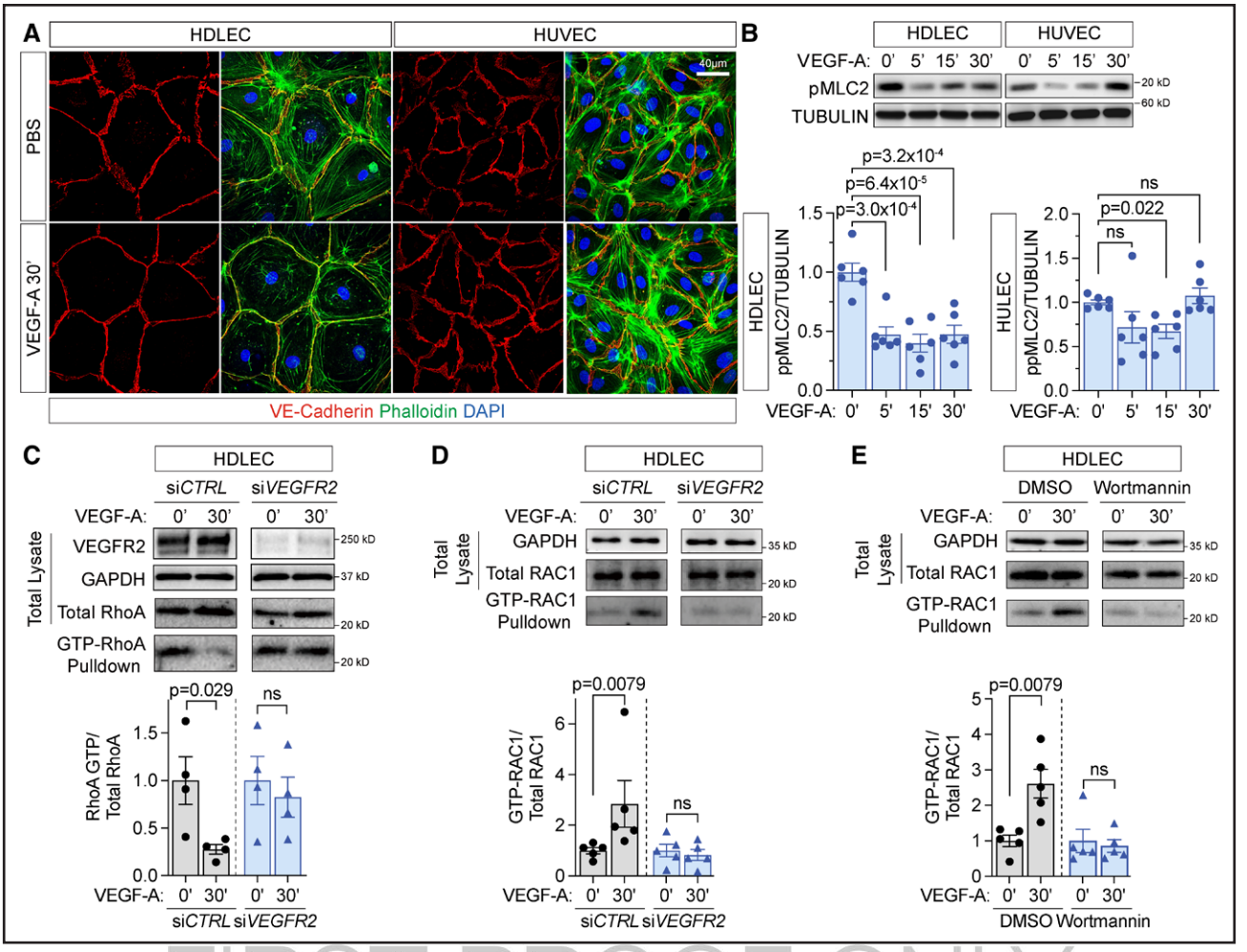

Figure 7. VEGF (vascular endothelial growth factor)-A/VEGFR (VEGF receptor) 2 inhibits stress fiber formation in human dermal lymphatic endothelial cells (HDLECs).

A, VE-Cadherin (vascular endothelial cadherin) and phalloidin staining of confluent human umbilical vein endothelial cells (HUVECs) and HDLECs starved in 0.2% serum for 6 hours and treated with 50 ng/mL VEGF-A or PBS for 30 minutes. **B**, Western blot and quantification of pMLC2 (Thr18/Ser19), normalized to TUBULIN, in confluent HUVECs and HDLECs starved for 6 hours and stimulated with 50 ng/mL VEGF-A for 0, 5, 15, and 30 minutes. Data are expressed as fold changes compared with the average value of T=0′ of each cell group. N=6 experiments. Error bars, SEM. ns, not significant. One-Way ANOVA with post hoc Tukey test (for HDLEC), or Welch ANOVA with post hoc Dunnett T3 test (for HUVEC). **C** and **D**, RhoA and RAC1 pulldown assays in HDLECs transfected with *CTRL* or *VEGFR2* siRNA and treated with 50 ng/mL VEGF-A for 30 minutes. **Top**, Western blots of GTP-bound RhoA/RAC1 from the pulldown assay and total RhoA/RAC1 from total cell lysates. **Bottom**, Quantifications of the ratios of GTP-bound RhoA/RAC1 to total RhoA/RAC1. Data are expressed as fold changes compared with the average value of T=0′ of each siRNA-treated group. N=4–5 experiments. Error bars, SEM. Mann-Whitney *U* test. **E**, RAC1 pulldown assay in HDLECs after 5 hours of Wortmannin (1 μM) or DMSO treatment and 30 minutes VEGF-A (50 ng/mL) stimulation. Shown are Western blots (**top**) and quantification (bottom) of the ratios of GTP-bound RAC1 to total RAC1 from cell lysates. Data are expressed as fold changes compared with the average value of T=0′ of each treatment group. N=5 experiments. Error bars, SEM. Mann-Whitney *U* test.

into the footpads of adult mice. The dye was quickly absorbed by lymphatic capillaries and transported to the draining lymph node in control mice, whereas VEGF-A injection resulted in significantly reduced dye uptake (Figure 8F through 8G). We also observed a significant reduction in the intensity of Evans Blue-filled lymphatics connected to popliteal lymph nodes in the *Rock1/2iLKOs* (Figure 8H through 8J). These results show that ROCK regulates lymphatic junction transformation and solute uptake function across different lymphatic capillary beds.

DISCUSSION

Our work identifies a 2-pronged homeostatic mechanism that triggers lacteal junction opening in intestinal lacteals. Chylomicrons rapidly activate ROCK in LECs, which initiates the formation of junction-anchored stress fibers and generates the tension required to pull junctions apart (Figure 8Ki). A similar mechanism has been described in BECs during the formation of focal adherens junctions, which contain vinculin and partially unzip to increase blood vascular permeability. Focal adherens junctions

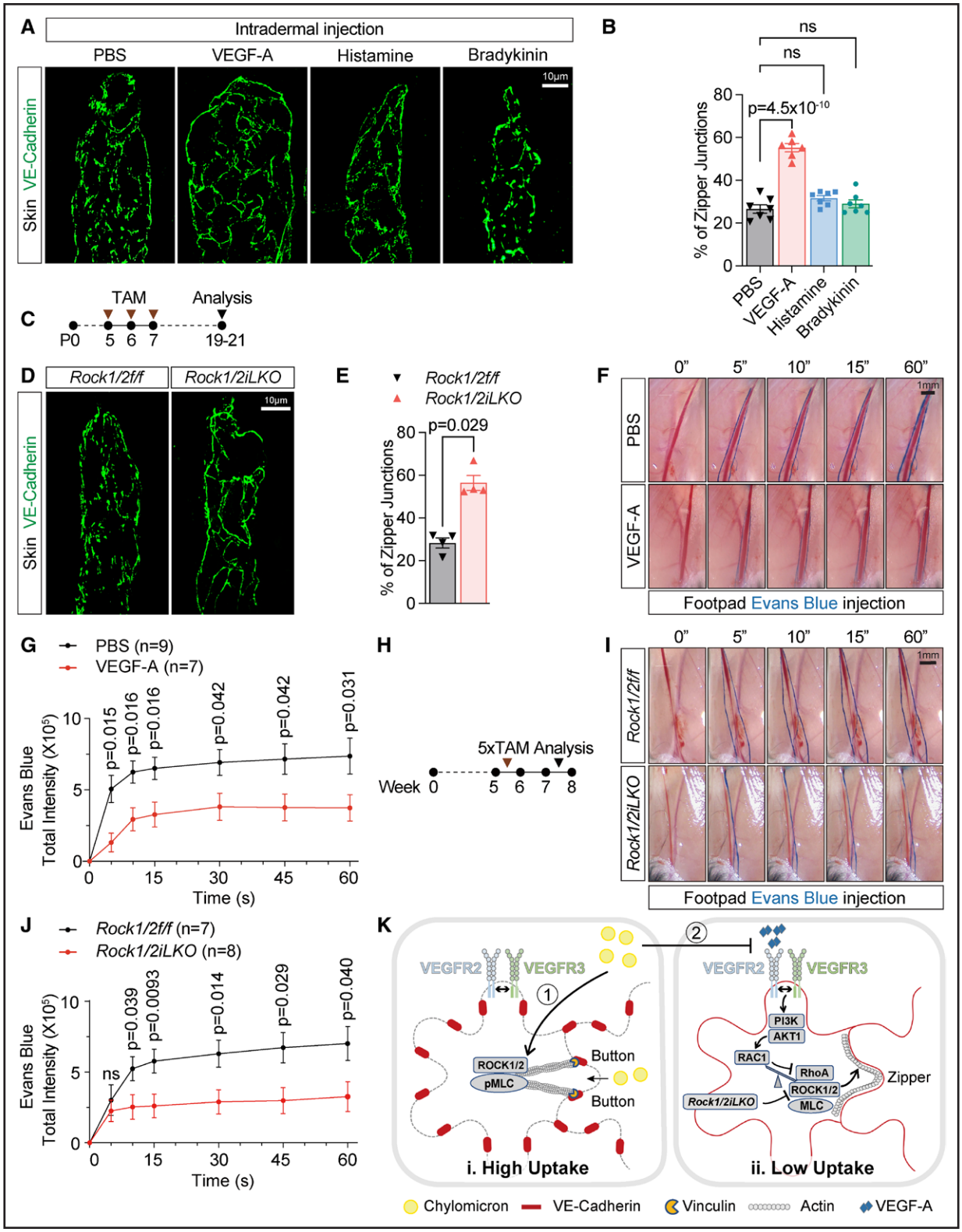

Figure 8. VEGF (vascular endothelial growth factor)-A and ROCK (Rho-associated kinase) signaling regulate dermal initial lymphatic drainage.

A, VE-Cadherin (vascular endothelial cadherin) staining of ear dermal initial lymphatics from postnatal day (P) 21 wild-type mice 30 minutes after intradermal injection of VEGF-A (50 ng in 20 μL PBS), histamine (500 ng in 20 μL PBS), bradykinin (20 μg in 20 μL PBS) or PBS alone. **B**, Quantification of % zipper-like lymphatic endothelial cell (LEC) junctions out of total lymphatic junction length in dermal initial lymphatics in **A**. Each symbol represents one mouse. N=6 or 7 mice per group. Error bars, SEM. ns, not significant. One-Way ANOVA with post hoc Tukey test. **C**, Experiment strategy to induce *Rock1/2* deletion shown in **D** and **E**. Arrowheads represent 3×75 μg/g tamoxifen (TAM) injections and (*Continued*)

formation requires actomyosin contractility and depends on RhoA GTPase activity.[47] Thus, RhoA and ROCK are key regulators of junctional morphology in both LECs and BECs.

We speculate that lipid activation of ROCK is a driving force that triggers cytoskeletal contraction and junction opening in the intestinal lacteal microenvironment. Lipids, such as lysophospholipids,[48,49] sphingolipids,[50] and fatty acids,[31–34] can activate GEFs (guanine nucleotide exchange factors) for RhoA through G-protein–coupled receptors and p38/MAPK. Arachidonic acids can also directly activate ROCK by binding to the autoinhibitory region of ROCK.[51] The mechanisms of ROCK activation in response to chylomicrons remains to be determined.

Following postnatal fat ingestion, VEGFR2 signaling is inhibited in the intestine. This is likely due to the chylomicron apolipoprotein $ApoB_{48}$ that could induce postnatal transcriptional upregulation of the VEGF-A decoy receptor VEGFR1 in BECs of the intestinal villi[8,18] (Figure 8Kii). VEGFR1 sequesters peri-lacteal VEGF-A and together with NRP1 (neuropilin 1) inhibits VEGFR2 signaling on LECs and junction zippering.[12] Therefore, chylomicrons take dual action to ensure perinatal lymphatic junction opening and their own intestinal absorption, which in mammals coincides with milk consumption immediately after birth.[31]

VEGF-A expression is tightly regulated in the microenvironment of the intestinal villi to maintain the fenestrated blood vasculature.[52] Increased VEGF-A bioavailability leads to vascular leakage in the intestinal villus,[8] which could indirectly affect LEC junctions. Here we show that the effects of VEGF-A on LEC junctions are neither a byproduct of concurrent BEC junction opening nor via effects on other cell types, such as mural cells.[53] Using VEGFR2 LEC-specific loss of function and gain-of-function mice, we show that VEGF-A antagonizes junction opening in a LEC-autonomous manner. VEGFR2 loss of function does not alter baseline junction morphology, in contrast to ROCK deletion, revealing antagonistic effects by VEGF-A and ROCK that are both controlled by chylomicrons.

We also show that VEGF-A-mediated inhibition of lacteal permeability is independent of Y949 but abolished by *VEGFR3* deletion. Since VEGFR3 does not bind VEGF-A directly, we conclude that VEGFR3 modulates VEGFR2 signaling output via VEGFR2/VEGFR3 heterodimers. Such heterodimers are formed in cultured LECs in response to VEGF-C,[42] as well as in BECs in angiogenic sprouts in response to VEGF-A and VEGF-C.[43] As VEGF-A–induced VEGFR2 Y951, Y1175, and Y1214 phosphorylation is unaffected by *VEGFR3* knockdown, the formation of such heterodimers may affect the sites of VEGFR3 tyrosine phosphorylation.[42,43]

VEGF-C-156S, a mutated form of VEGF-C that only binds VEGFR3,[54] was unable to zipper the lacteal junctions of control mice,[8] and VEGFR3 inhibition with monoclonal antibodies failed to reverse zippered junctions in the inflamed mouse trachea.[6] However, VEGF-C produced by lacteal macrophages in response to microbial stimuli is required for button maintenance.[12] We suggest that these effects are mediated by VEGFR2, or via VEGFR2/VEGFR3 heterodimers, since proteolytically processed VEGF-C also binds to and activates VEGFR2.[55] *VEGFR3* knockdown abolished AKT activation downstream of VEGF-A in HDLECs, and AKT deletion prevented VEGF-A–induced lacteal junction zippering in vivo. Conversely, *VEGFR2* knockdown in LECs prevents VEGF-C–induced AKT phosphorylation, but not ERK activation.[56] Taken together, the data are consistent with a model where VEGF-A or VEGF-C induced VEGFR2/VEGFR3 heterodimer signaling to AKT accounts for LEC permeability inhibition.

VEGF-A–mediated activation of VEGFR2 zippered lacteal junctions by suppressing RhoA via increased RAC1 activation (Figure 8Kii). RAC1 antagonizes RhoA to remodel apical junctions as described in a variety of cellular contexts.[57] In this case, RAC1 inhibits RhoA, whereas RhoA can in turn restrain RAC1 activity. Interestingly, in BECs, signaling via VEGFR2 leads to activation of both RAC1[58–60] and RhoA,[61] suggesting that the dynamics of pathway activation are different in BECs

Figure 8 Continued. analysis at P19–P21. **D** and **E**, VE-Cadherin staining and quantification of % zipper-like junctions out of total junction length in ear dermal initial lymphatics from P19 to P21 *Rock1/2f/f* and *Rock1/2iLKO* mice. Each symbol represents one mouse. N=4 mice per group. Error bars, SEM. Mann-Whitney *U* test. **F**, Evans Blue absorption in lower leg lymphatic vessels of adult wild-type mice at the indicated time points after footpad injection of VEGF-A (20 ng in 5 µL PBS) or PBS alone, and 5 µL of 1.5% Evans Blue solution. **G**, Quantification of dye intensity in Evans Blue-filled lymphatics in **F**. N=7 or 9 mice per group. Error bars, SEM. Mann-Whitney *U* test was performed to compare PBS and VEGF-A–treated groups at the same time points. **H**, Timeline of TAM administration (2 mg per day for 5 days) of adult *Rock1/2f/f* and *Rock1/2iLKO* mice. All mice were analyzed 10 days after the last TAM injection. **I**, Evans Blue uptake in lower leg lymphatic vessels of *Rock1/2f/f* and *Rock1/2iLKO* mice at the indicated time points after intradermal footpad injection of 9 µL 1.5% Evans Blue solution. **J**, Quantification of dye intensity in Evans Blue-filled lymphatics in **I**. N=7–8 mice per group. Error bars, SEM. Mann-Whitney *U* test was performed to compare *Rock1/2f/f* and *Rock1/2iLKO* mouse groups at the same time points. **K**, Summary model of LEC junction remodeling in intestinal lacteals. **Ki.** High lipid uptake: chylomicrons derived from ingested lipids activate ROCK (1), which phosphorylates MLC2 (myosin light chain 2) and induces actomyosin stress fiber assembly and junction opening, thereby enabling lacteal chylomicron uptake. VEGFR (vascular endothelial growth factor receptor) 2 is inhibited by chylomicron upregulation of VEGFR1 and NRP1 (neuropilin 1) in blood vascular endothelial cells, which reduces VEGF-A signals to LEC VEGFR2 (2). **Kii.** Low lipid uptake: VEGF-A signals via VEGFR2/VEGFR3 heterodimers to antagonize ROCK activation and junction opening. VEGFR2/VEGFR3 activate RAC1 via PI3K/AKT, thereby reducing RhoA and ROCK-dependent MLC2 phosphorylation, resulting in actin stress fiber relaxation, cortical actin formation, and junction zippering, which prevents chylomicron uptake by lacteals.

versus LECs. PI3K/AKT signaling can activate RAC1 in many cell types,[62–64] but how exactly PI3K activation downstream of VEGF-A/VEGFR2 results in activation of RAC1 in LECs remains to be determined.

ROCK deletion resulted ultimately in lethality in the *Rock1/2iLKO* mice. Determining the cause of death requires further investigation. *Prox1CreERT2* is expressed also in other cell types, such as hepatocytes, cardiomyocytes, and some neuronal cells and, therefore, we cannot exclude off-target effects of ROCK loss of function that could underlie the increased mortality of the mutants.

Finally, we show that ROCK activity is essential for button formation also outside of the gastrointestinal tract. The upstream signaling pathways activating ROCK in skin lymphatics remain to be determined. Dexamethasone activation of LEC glucocorticoid receptors, which increase RhoA-mediated contractility in various settings[65,66] promotes button formation and decreases edema in inflamed tracheal lymphatics.[6] It is, therefore, likely that signaling through glucocorticoid receptor or other surface receptors, such as *Calcrl*, TGFβR (TGF [transforming growth factor] β-receptor), PDFGR (platelet-derived growth factor receptor), and EGFR (epidermal growth factor receptor) that also activate RhoA, may contribute to button formation in different tissues.[67–69] Other environmental inputs, including enzymes such as thrombin,[70] flow shear,[71] and mechanical forces[72] may also be at play. Understanding the inputs into the cytoskeletal mechanism that we here uncover could allow manipulation of lymphatic permeability to control tissue drainage and immune cell trafficking in preclinical disease models.

ARTICLE INFORMATION

Received January 31, 2023; revision received June 30, 2023; accepted July 6, 2023.

Affiliations

Cardiovascular Research Center and Department of Cellular and Molecular Physiology, Yale University School of Medicine, New Haven, CT (G.Z., M.L., D.C., N.R., M.S., A.E.). State Key Laboratory of Ophthalmology, Zhongshan Ophthalmic Center, Sun Yat-sen University, Guangdong Provincial Key Laboratory of Ophthalmology and Visual Science, Guangzhou, China (X.C., X. Zhou, L.Z., W.L., X. Zhang, Y.L., W.Z., K.L., R.J., X.L., F.Z.). University of Arizona, College of Medicine, Banner University Medical Center, Tucson (J.L.). Division of Endocrinology, Diabetes and Metabolism, Beth Israel Deaconess Medical Center and Harvard Medical School, Boston, MA (Y.-B.K.). Molecular Genetics of Angiogenesis Group, Centro Nacional de Investigaciones Cardiovasculares (CNIC), Madrid, Spain (R.B.). Uppsala University, Rudbeck, SciLifeLab and Beijer Laboratories, Department of Immunology, Genetics and Pathology, Sweden (L.C.-W.). Wihuri Research Institute and Translational Cancer Medicine Program, Biomedicum, University of Helsinki, Finland (K.A.). INSERM U970, Paris Cardiovascular Research Center, France (A.E.). Now with Department of Physiology and Neurobiology, University of Connecticut, Storrs (G.Z.).

Acknowledgments

The authors thank Drs J.-L. Thomas and A. Dubrac for discussion and J. Luo, S. Yi, and M. Zhang for technical assistance. G. Zarkada, M. Simons, A. Eichmann, and F. Zhang contributed to study design. G. Zarkada, X. Chen, X. Zhou, M. Lange, L. Zeng, X. Zhang, Y. Li, W. Lv, X. Zhou, W. Zhou, D. Chen, N. Ricard, XG, and F. Zhang conducted the experiments. G. Zarkada, X. Chen, K. Liu, M. Lange, X. Zhou, W. Lv, X. Zhang, W. Zhou, L. Zeng, XG, R. Ju, X. Li, A. Eichmann, and F. Zhang participated in data analysis. J. Liao, Y.-B. Kim, R. Benedito, L. Claesson-Welsh, K. Alitalo, M. Simons contributed to material provision. G. Zarkada, X. Chen, K. Alitalo, R. Ju, X. Li, A. Eichmann, and F. Zhang contributed to article writing and editing. J. Liao, Y.-B. Kim, R. Benedito, L. Claesson-Welsh, and M. Simons reviewed the article.

Sources of Funding

This project was supported by grants from National Key R&D Program of China (2021YFA1101200), National Natural Science Foundation of China (82070500, 82241009), Natural Science Foundation of Guangdong Province (2022A1515012210), and the Science and Technology Program of Guangzhou City (202102010183) to F. Zhang, and from National Institutes of Health (NIH; 1R01DK120373-01A1) and the Leducq Foundation (TNE ATTRACT) to A. Eichmann.

Disclosures

None.

Supplemental Material

Figure S1–S5
Supplementary Methods
Major Resources Table
Uncropped Immunoblots File

REFERENCES

1. Jackson DG. Leucocyte trafficking via the lymphatic vasculature-mechanisms and consequences. *Front Immunol.* 2019;10:471. doi: 10.3389/fimmu.2019.00471
2. Cifarelli V, Eichmann A. The intestinal lymphatic system: functions and metabolic implications. *Cell Mol Gastroenterol Hepatol.* 2019;7:503–513. doi: 10.1016/j.jcmgh.2018.12.002
3. Petrova TV, Koh GY. Organ-specific lymphatic vasculature: from development to pathophysiology. *J Exp Med.* 2018;215:35–49. doi: 10.1084/jem.20171868
4. Baluk P, Fuxe J, Hashizume H, Romano T, Lashnits E, Butz S, Vestweber D, Corada M, Molendini C, Dejana E, et al. Functionally specialized junctions between endothelial cells of lymphatic vessels. *J Exp Med.* 2007;204:2349–2362. doi: 10.1084/jem.20062596
5. Zhang F, Zarkada G, Yi S, Eichmann A. Lymphatic endothelial cell junctions: molecular regulation in physiology and diseases. *Front Physiol.* 2020;11:509. doi: 10.3389/fphys.2020.00509
6. Yao LC, Baluk P, Srinivasan RS, Oliver G, McDonald DM. Plasticity of button-like junctions in the endothelium of airway lymphatics in development and inflammation. *Am J Pathol.* 2012;180:2561–2575. doi: 10.1016/j.ajpath.2012.02.019
7. Churchill MJ, du Bois H, Heim TA, Mudianto T, Steele MM, Nolz JC, Lund AW. Infection-induced lymphatic zippering restricts fluid transport and viral dissemination from skin. *J Exp Med.* 2022;219:e20211830. doi: 10.1084/jem.20211830
8. Zhang F, Zarkada G, Han J, Li J, Dubrac A, Ola R, Genet G, Boye K, Michon P, Kunzel SE, et al. Lacteal junction zippering protects against diet-induced obesity. *Science.* 2018;361:599–603. doi: 10.1126/science.aap9331
9. Koletzko B. Human milk lipids. *Ann Nutr Metab.* 2016;69(Suppl 2):28–40. doi: 10.1159/000452819
10. Randolph GJ, Miller NE. Lymphatic transport of high-density lipoproteins and chylomicrons. *J Clin Invest.* 2014;124:929–935. doi: 10.1172/JCI71610
11. Nurmi H, Saharinen P, Zarkada G, Zheng W, Robciuc MR, Alitalo K. VEGF-C is required for intestinal lymphatic vessel maintenance and lipid absorption. *EMBO Mol Med.* 2015;7:1418–1425. doi: 10.15252/emmm.201505731
12. Suh SH, Choe K, Hong SP, Jeong SH, Makinen T, Kim KS, Alitalo K, Surh CD, Koh GY, Song JH. Gut microbiota regulates lacteal integrity by inducing VEGF-C in intestinal villus macrophages. *EMBO Rep.* 2019;20:e46927. doi: 10.15252/embr.201846927
13. Hong SP, Yang MJ, Cho H, Park I, Bae H, Choe K, Suh SH, Adams RH, Alitalo K, Lim D, et al. Distinct fibroblast subsets regulate lacteal integrity through YAP/TAZ-induced VEGF-C in intestinal villi. *Nat Commun.* 2020;11:4102. doi: 10.1038/s41467-020-17886-y
14. Shew T, Wolins NE, Cifarelli V. VEGFR-3 signaling regulates triglyceride retention and absorption in the intestine. *Front Physiol.* 2018;9:1783. doi: 10.3389/fphys.2018.01783
15. Bernier-Latmani J, Cisarovsky C, Demir CS, Bruand M, Jaquet M, Davanture S, Ragusa S, Siegert S, Dormond O, Benedito R, et al. DLL4 promotes continuous adult intestinal lacteal regeneration and dietary fat transport. *J Clin Invest.* 2015;125:4572–4586. doi: 10.1172/JCI82045

16. Davis RB, Kechele DO, Blakeney ES, Pawlak JB, Caron KM. Lymphatic deletion of calcitonin receptor-like receptor exacerbates intestinal inflammation. *JCI Insight*. 2017;2:e92465. doi: 10.1172/jci.insight.92465
17. Hu S, Mahadevan A, Elysee IF, Choi J, Souchet NR, Bae GH, Taboada AK, Sanketi B, Duhamel GE, Sevier CS, et al. The asymmetric Pitx2 gene regulates gut muscular-lacteal development and protects against fatty liver disease. *Cell Rep*. 2021;37:110030. doi: 10.1016/j.celrep.2021.110030
18. Avraham-Davidi I, Ely Y, Pham VN, Castranova D, Grunspan M, Malkinson G, Gibbs-Bar L, Mayseless O, Allmog G, Lo B, et al. ApoB-containing lipoproteins regulate angiogenesis by modulating expression of VEGF receptor 1. *Nat Med*. 2012;18:967–973. doi: 10.1038/nm.2759
19. Li X, Padhan N, Sjostrom EO, Roche FP, Testini C, Honkura N, Sainz-Jaspeado M, Gordon E, Bentley K, Philippides A, et al. VEGFR2 pY949 signalling regulates adherens junction integrity and metastatic spread. *Nat Commun*. 2016;7:11017. doi: 10.1038/ncomms11017
20. Cho H, Thorvaldsen JL, Chu Q, Feng F, Birnbaum MJ. Akt1/PKBalpha is required for normal growth but dispensable for maintenance of glucose homeostasis in mice. *J Biol Chem*. 2001;276:38349–38352. doi: 10.1074/jbc.C100462200
21. Hooper AT, Butler JM, Nolan DJ, Kranz A, Iida K, Kobayashi M, Kopp HG, Shido K, Petit I, Yanger K, et al. Engraftment and reconstitution of hematopoiesis is dependent on VEGFR2-mediated regeneration of sinusoidal endothelial cells. *Cell Stem Cell*. 2009;4:263–274. doi: 10.1016/j.stem.2009.01.006
22. Haiko P, Makinen T, Keskitalo S, Taipale J, Karkkainen MJ, Baldwin ME, Stacker SA, Achen MG, Alitalo K. Deletion of vascular endothelial growth factor C (VEGF-C) and VEGF-D is not equivalent to VEGF receptor 3 deletion in mouse embryos. *Mol Cell Biol*. 2008;28:4843–4850. doi: 10.1128/MCB.02214-07
23. Fu G, Chen Y, Yu M, Podd A, Schuman J, He Y, Di L, Yassai M, Haribhai D, North PE, et al. Phospholipase C{gamma}1 is essential for T cell development, activation, and tolerance. *J Exp Med*. 2010;207:309–318. doi: 10.1084/jem.20090880
24. Huang H, Kong D, Byun KH, Ye C, Koda S, Lee DH, Oh BC, Lee SW, Lee B, Zabolotny JM, et al. Rho-kinase regulates energy balance by targeting hypothalamic leptin receptor signaling. *Nat Neurosci*. 2012;15:1391–1398. doi: 10.1038/nn.3207
25. Okamoto R, Li Y, Noma K, Hiroi Y, Liu PY, Taniguchi M, Ito M, Liao JK. FHL2 prevents cardiac hypertrophy in mice with cardiac-specific deletion of ROCK2. *FASEB J*. 2013;27:1439–1449. doi: 10.1096/fj.12-217018
26. Kumper S, Mardakheh FK, McCarthy A, Yeo M, Stamp GW, Paul A, Worboys J, Sadok A, Jorgensen C, Guichard S, et al. Rho-associated kinase (ROCK) function is essential for cell cycle progression, senescence and tumorigenesis. *Elife*. 2016;5:e12994. doi: 10.7554/eLife.12203
27. Pontes-Quero S, Heredia L, Casquero-Garcia V, Fernandez-Chacon M, Luo W, Hermoso A, Bansal M, Garcia-Gonzalez I, Sanchez-Munoz MS, Perea JR, et al. Dual ifgMosaic: a versatile method for multispectral and combinatorial mosaic gene-function analysis. *Cell*. 2017;170:800–814.e18. doi: 10.1016/j.cell.2017.07.031
28. Bazigou E, Lyons OT, Smith A, Venn GE, Cope C, Brown NA, Makinen T. Genes regulating lymphangiogenesis control venous valve formation and maintenance in mice. *J Clin Invest*. 2011;121:2984–2992. doi: 10.1172/JCI58050
29. Salem N Jr, Van Dael P. Arachidonic acid in human milk. *Nutrients*. 2020;12:626. doi: 10.3390/nu12030626
30. Garcia MC, Ray DM, Lackford B, Rubino M, Olden K, Roberts JD. Arachidonic acid stimulates cell adhesion through a novel p38 MAPK-RhoA signaling pathway that involves heat shock protein 27. *J Biol Chem*. 2009;284:20936–20945. doi: 10.1074/jbc.M109.020271
31. Feng J, Ito M, Kureishi Y, Ichikawa K, Amano M, Isaka N, Okawa K, Iwamatsu A, Kaibuchi K, Hartshorne DJ, et al. Rho-associated kinase of chicken gizzard smooth muscle. *J Biol Chem*. 1999;274:3744–3752. doi: 10.1074/jbc.274.6.3744
32. Dietze R, Hammoud MK, Gomez-Serrano M, Unger A, Bieringer T, Finkernagel F, Sokol AM, Nist A, Stiewe T, Reinartz S, et al. Phosphoproteomics identify arachidonic-acid-regulated signal transduction pathways modulating macrophage functions with implications for ovarian cancer. *Theranostics*. 2021;11:1377–1395. doi: 10.7150/thno.52442
33. George MD, Wine RN, Lackford B, Kissling GE, Akiyama SK, Olden K, Roberts JD. p38 mitogen-activated protein kinase interacts with vinculin at focal adhesions during fatty acid-stimulated cell adhesion. *Biochem Cell Biol*. 2013;91:404–418. doi: 10.1139/bcb-2013-0013
34. Garcia MC, Williams J, Johnson K, Olden K, Roberts JD. Arachidonic acid stimulates formation of a novel complex containing nucleolin and RhoA. *FEBS Lett*. 2011;585:618–622. doi: 10.1016/j.febslet.2011.01.035
35. Loirand G. Rho kinases in health and disease: from basic science to translational research. *Pharmacol Rev*. 2015;67:1074–1095. doi: 10.1124/pr.115.010595
36. Sun Z, Li X, Massena S, Kutschera S, Padhan N, Gualandi L, Sundvold-Gjerstad V, Gustafsson K, Choy WW, Zang G, et al. VEGFR2 induces c-Src signaling and vascular permeability in vivo via the adaptor protein TSAd. *J Exp Med*. 2012;209:1363–1377. doi: 10.1084/jem.20111343
37. Orsenigo F, Giampietro C, Ferrari A, Corada M, Galaup A, Sigismund S, Ristagno G, Maddaluno L, Koh GY, Franco D, et al. Phosphorylation of VE-cadherin is modulated by haemodynamic forces and contributes to the regulation of vascular permeability in vivo. *Nat Commun*. 2012;3:1208. doi: 10.1038/ncomms2199
38. Jin Y, Ding Y, Richards M, Kaakinen M, Giese W, Baumann E, Szymborska A, Rosa A, Nordling S, Schimmel L, et al. Tyrosine-protein kinase Yes controls endothelial junctional plasticity and barrier integrity by regulating VE-cadherin phosphorylation and endocytosis. *Nature Cardiovascular Research*. 2022;1:1156–1173. doi: 10.1038/s44161-022-00172-z
39. Vaahtomeri K, Karaman S, Makinen T, Alitalo K. Lymphangiogenesis guidance by paracrine and pericellular factors. *Genes Dev*. 2017;31:1615–1634. doi: 10.1101/gad.303776.117
40. Koch S, Tugues S, Li X, Gualandi L, Claesson-Welsh L. Signal transduction by vascular endothelial growth factor receptors. *Biochem J*. 2011;437:169–183. doi: 10.1042/BJ20110301
41. Zarkada G, Heinolainen K, Makinen T, Kubota Y, Alitalo K. VEGFR3 does not sustain retinal angiogenesis without VEGFR2. *Proc Natl Acad Sci U S A*. 2015;112:761–766. doi: 10.1073/pnas.1423278112
42. Dixelius J, Makinen T, Wirzenius M, Karkkainen MJ, Wernstedt C, Alitalo K, Claesson-Welsh L. Ligand-induced vascular endothelial growth factor receptor-3 (VEGFR-3) heterodimerization with VEGFR-2 in primary lymphatic endothelial cells regulates tyrosine phosphorylation sites. *J Biol Chem*. 2003;278:40973–40979. doi: 10.1074/jbc.M304499200
43. Nilsson I, Bahram F, Li X, Gualandi L, Koch S, Jarvius M, Soderberg O, Anisimov A, Kholova I, Pytowski B, et al. VEGF receptor 2/-3 heterodimers detected in situ by proximity ligation on angiogenic sprouts. *EMBO J*. 2010;29:1377–1388. doi: 10.1038/emboj.2010.30
44. Chen D, Simons M. Emerging roles of PLCgamma1 in endothelial biology. *Sci Signal*. 2021;14:eabc6612. doi: 10.1126/scisignal.abc6612
45. Cifarelli V, Appak-Baskoy S, Peche VS, Kluzak A, Shew T, Narendran R, Pietka KM, Cella M, Walls CW, Czepielewski R, et al. Visceral obesity and insulin resistance associate with CD36 deletion in lymphatic endothelial cells. *Nat Commun*. 2021;12:3350. doi: 10.1038/s41467-021-23808-3
46. Guilluy C, Garcia-Mata R, Burridge K. Rho protein crosstalk: another social network? *Trends Cell Biol*. 2011;21:718–726. doi: 10.1016/j.tcb.2011.08.002
47. Huveneers S, Oldenburg J, Spanjaard E, van der Krogt G, Grigoriev I, Akhmanova A, Rehmann H, de Rooij J. Vinculin associates with endothelial VE-cadherin junctions to control force-dependent remodeling. *J Cell Biol*. 2012;196:641–652. doi: 10.1083/jcb.201108120
48. Skoura A, Hla T. Regulation of vascular physiology and pathology by the S1P2 receptor subtype. *Cardiovasc Res*. 2009;82:221–228. doi: 10.1093/cvr/cvp088
49. Xiang SY, Dusaban SS, Brown JH. Lysophospholipid receptor activation of RhoA and lipid signaling pathways. *Biochim Biophys Acta*. 2013;1831:213–222. doi: 10.1016/j.bbalip.2012.09.004
50. Singh RK, Haka AS, Brumfield A, Grosheva I, Bhardwaj P, Chin HF, Xiong Y, Hla T, Maxfield FR. Ceramide activation of RhoA/Rho kinase impairs actin polymerization during aggregated LDL catabolism. *J Lipid Res*. 2017;58:1977–1987. doi: 10.1194/jlr.M076398
51. Araki S, Ito M, Kureishi Y, Feng J, Machida H, Isaka N, Amano M, Kaibuchi K, Hartshorne DJ, Nakano T. Arachidonic acid-induced Ca2+ sensitization of smooth muscle contraction through activation of Rho-kinase. *Pflugers Arch*. 2001;441:596–603. doi: 10.1007/s004240000462
52. Bernier-Latmani J, Mauri C, Marcone R, Renevey F, Durot S, He L, Vanlandewijck M, Maclachlan C, Davanture S, Zamboni N, et al. ADAMTS18(+) villus tip telocytes maintain a polarized VEGFA signaling domain and fenestrations in nutrient-absorbing intestinal blood vessels. *Nat Commun*. 2022;13:3983. doi: 10.1038/s41467-022-31571-2
53. Ishida A, Murray J, Saito Y, Kanthou C, Benzakour O, Shibuya M, Wijelath ES. Expression of vascular endothelial growth factor receptors in smooth muscle cells. *J Cell Physiol*. 2001;188:359–368. doi: 10.1002/jcp.1121
54. Joukov V, Kumar V, Sorsa T, Arighi E, Weich H, Saksela O, Alitalo K. A recombinant mutant vascular endothelial growth factor-C that has lost vascular endothelial growth factor receptor-2 binding, activation, and vascular permeability activities. *J Biol Chem*. 1998;273:6599–6602. doi: 10.1074/jbc.273.12.6599

55. Joukov V, Sorsa T, Kumar V, Jeltsch M, Claesson-Welsh L, Cao Y, Saksela O, Kalkkinen N, Alitalo K. Proteolytic processing regulates receptor specificity and activity of VEGF-C. *EMBO J*. 1997;16:3898–3911. doi: 10.1093/emboj/16.13.3898
56. Deng Y, Zhang X, Simons M. Molecular controls of lymphatic VEGFR3 signaling. *Arterioscler Thromb Vasc Biol*. 2015;35:421–429. doi: 10.1161/ATVBAHA.114.304881
57. Nguyen LK, Kholodenko BN, von Kriegsheim A. Rac1 and RhoA: networks, loops and bistability. *Small GTPases*. 2018;9:316–321. doi: 10.1080/21541248.2016.1224399
58. Oshikawa J, Kim SJ, Furuta E, Caliceti C, Chen GF, McKinney RD, Kuhr F, Levitan I, Fukai T, Ushio-Fukai M. Novel role of p66Shc in ROS-dependent VEGF signaling and angiogenesis in endothelial cells. *Am J Physiol Heart Circ Physiol*. 2012;302:H724–H732. doi: 10.1152/ajpheart.00739.2011
59. Wang H, Ramshekar A, Kunz E, Sacks DB, Hartnett ME. IQGAP1 causes choroidal neovascularization by sustaining VEGFR2-mediated Rac1 activation. *Angiogenesis*. 2020;23:685–698. doi: 10.1007/s10456-020-09740-y
60. Monaghan-Benson E, Hartmann J, Vendrov AE, Budd S, Byfield G, Parker A, Ahmad F, Huang W, Runge M, Burridge K, et al. The role of vascular endothelial growth factor-induced activation of NADPH oxidase in choroidal endothelial cells and choroidal neovascularization. *Am J Pathol*. 2010;177:2091–2102. doi: 10.2353/ajpath.2010.090878
61. Graupera M, Guillermet-Guibert J, Foukas LC, Phng LK, Cain RJ, Salpekar A, Pearce W, Meek S, Millan J, Cutillas PR, et al. Angiogenesis selectively requires the p110alpha isoform of PI3K to control endothelial cell migration. *Nature*. 2008;453:662–666. doi: 10.1038/nature06892
62. Han J, Luby-Phelps K, Das B, Shu X, Xia Y, Mosteller RD, Krishna UM, Falck JR, White MA, Broek D. Role of substrates and products of PI 3-kinase in regulating activation of Rac-related guanosine triphosphatases by Vav. *Science*. 1998;279:558–560. doi: 10.1126/science.279.5350.558
63. Rodriguez-Viciana P, Warne PH, Khwaja A, Marte BM, Pappin D, Das P, Waterfield MD, Ridley A, Downward J. Role of phosphoinositide 3-OH kinase in cell transformation and control of the actin cytoskeleton by Ras. *Cell*. 1997;89:457–467. doi: 10.1016/s0092-8674(00)80226-3
64. Zhu G, Fan Z, Ding M, Zhang H, Mu L, Ding Y, Zhang Y, Jia B, Chen L, Chang Z, et al. An EGFR/PI3K/AKT axis promotes accumulation of the Rac1-GEF Tiam1 that is critical in EGFR-driven tumorigenesis. *Oncogene*. 2015;34:5971–5982. doi: 10.1038/onc.2015.45
65. Wang HL, Yang CH, Lee HH, Kuo JC, Hur SS, Chien S, Lee OK, Hung SC, Chang ZF. Dexamethasone-induced cellular tension requires a SGK1-stimulated Sec5-GEF-H1 interaction. *J Cell Sci*. 2015;128:3757–3768. doi: 10.1242/jcs.169961
66. Fujimoto T, Inoue T, Kameda T, Kasaoka N, Inoue-Mochita M, Tsuboi N, Tanihara H. Involvement of RhoA/Rho-associated kinase signal transduction pathway in dexamethasone-induced alterations in aqueous outflow. *Invest Ophthalmol Vis Sci*. 2012;53:7097–7108. doi: 10.1167/iovs.12-9989
67. Tripathi BK, Grant T, Qian X, Zhou M, Mertins P, Wang D, Papageorge AG, Tarasov SG, Hunter KW, Carr SA, et al. Receptor tyrosine kinase activation of RhoA is mediated by AKT phosphorylation of DLC1. *J Cell Biol*. 2017;216:4255–4270. doi: 10.1083/jcb.201703105
68. Peng F, Zhang B, Wu D, Ingram AJ, Gao B, Krepinsky JC. TGFbeta-induced RhoA activation and fibronectin production in mesangial cells require caveolae. *Am J Physiol Renal Physiol*. 2008;295:F153–F164. doi: 10.1152/ajprenal.00419.2007
69. Tang L, Dai F, Liu Y, Yu X, Huang C, Wang Y, Yao W. RhoA/ROCK signaling regulates smooth muscle phenotypic modulation and vascular remodeling via the JNK pathway and vimentin cytoskeleton. *Pharmacol Res*. 2018;133:201–212. doi: 10.1016/j.phrs.2018.05.011
70. van Nieuw Amerongen GP, van Delft S, Vermeer MA, Collard JG, van Hinsbergh VW. Activation of RhoA by thrombin in endothelial hyperpermeability: role of Rho kinase and protein tyrosine kinases. *Circ Res*. 2000;87:335–340. doi: 10.1161/01.res.87.4.335
71. Norden PR, Sabine A, Wang Y, Demir CS, Liu T, Petrova TV, Kume T. Shear stimulation of FOXC1 and FOXC2 differentially regulates cytoskeletal activity during lymphatic valve maturation. *Elife*. 2020;9:e53814. doi: 10.7554/eLife.53814
72. Lessey EC, Guilluy C, Burridge K. From mechanical force to RhoA activation. *Biochemistry*. 2012;51:7420–7432. doi: 10.1021/bi300758e